

A Review of Electric Potential-Controlled Boundary Lubrication

Shaowei Li ^{1,*}, Chenxu Liu ², Wang He ¹, Jie Zhang ¹, Xiaoxi Qiao ¹, Jiang Li ¹, Dong Xiang ¹, Gao Qian ³, Pengpeng Bai ², Yonggang Meng ² and Yu Tian ^{2,*}

¹ School of Mechanical Engineering, University of Science and Technology Beijing, Beijing 100083, China; hewang1998@outlook.com (W.H.); zhangj517@ustb.edu.cn (J.Z.); qiaoxiaoxi@ustb.edu.cn (X.Q.); lijiang@ustb.edu.cn (J.L.); xdustb@163.com (D.X.)

² State Key Laboratory of Tribology in Advanced Equipment, Tsinghua University, Beijing 100084, China; liuchenxu19910407@163.com (C.L.); baipengpeng@mail.tsinghua.edu.cn (P.B.); mengyg@tsinghua.edu.cn (Y.M.)

³ The Institute of Service-Oriented Manufacturing Co., Ltd., Hangzhou 311103, China; qiango@isom.org.cn

* Correspondence: swli819@ustb.edu.cn (S.L.); tianyu@mail.tsinghua.edu.cn (Y.T.)

Abstract: Tribotronics represents the modulation of friction via an external electric potential, a field with promising ramifications for intelligent devices, precision manufacturing, and biomedical applications. A profound elucidation of mechanisms that allow for potential-controlled friction is foundational to further research in this tribotronic domain. This article provides a comprehensive review of the research progress in electro-controlled friction over the past few decades, approached from the perspective of the boundary lubrication film at the friction interface, a direct influencer of electro-controlled friction performance. The mechanisms of potential-controlled friction are categorized into three distinct classifications, contingent on the formation mode of the boundary lubrication film: potential-induced interfacial redox reactions, interfacial physical adsorption, and interfacial phase structure transformations. Furthermore, an outlook on the application prospects of electro-controlled friction is provided. Finally, several research directions worth exploring in the field of electro-controlled friction are proposed. The authors hope that this article will further promote the application of electro-controlled friction technology in engineering and provide intellectual inspiration for related researchers.

Keywords: tribotronic; interfacial interaction; redox; physisorption; structure transformations



Citation: Li, S.; Liu, C.; He, W.; Zhang, J.; Qiao, X.; Li, J.; Xiang, D.; Qian, G.; Bai, P.; Meng, Y.; et al. A Review of Electric Potential-Controlled Boundary Lubrication. *Lubricants* **2023**, *11*, 467. <https://doi.org/10.3390/lubricants11110467>

Received: 26 September 2023

Revised: 21 October 2023

Accepted: 28 October 2023

Published: 31 October 2023



Copyright: © 2023 by the authors. Licensee MDPI, Basel, Switzerland. This article is an open access article distributed under the terms and conditions of the Creative Commons Attribution (CC BY) license (<https://creativecommons.org/licenses/by/4.0/>).

1. Introduction

Friction is ubiquitous in daily life and industrial manufacturing, arising when two contact surfaces slide against one another. This interaction can lead to wear and tear on machinery and equipment, potentially causing premature failure or diminished accuracy [1,2]. Yet, friction remains integral to human activities and productivity. For instance, locomotion in humans and animals necessitates friction between limbs and terrain, just as the operation of vehicles and railways hinges on friction for torque transmission. In recent years, the increasing sophistication and digitalization of electromechanical products have necessitated not only the reduction or enhancement of friction but also its real-time active control. Designing a high-precision, rapidly adjustable friction control system is paramount for advancing cutting-edge equipment. Active friction control methods encompass load adjustments [2,3], lubricant application [4–8], and external field manipulation [9,10]. While load modifications necessitate supplementary control mechanisms, increasing machinery complexity, lubricants can reduce friction between moving surfaces but fail to offer reversible friction control or preset friction coefficient (COF) magnitudes. By contrast, external field stimulation allows for reversible active friction control without added mechanical intricacy. Common external field control techniques include electric potential control [11,12], magnetic field manipulation [13–15], and temperature regulation [16–18].

Of these methods, electric potential control is regarded as the most promising approach for achieving high-precision and rapid active friction control [19,20]. This is attributed to the real-time adjustability of electrode surface properties in potential control systems, enabling swift transitions in friction characteristics. Furthermore, in an electrochemical system maintaining constant potential, electrode surface properties can be preserved for extended periods, offering the potential for precise friction control through voltage manipulation.

The Stribeck curve delineates three distinct lubrication regimes: hydrodynamic, mixed, and boundary lubrication. Hydrodynamic lubrication and boundary lubrication represent two quintessential states of lubrication [21,22], as depicted in Figure 1. In the state of hydrodynamic lubrication, two solid surfaces are entirely separated by a consistent fluid film [23], with the external load being fully supported by this film. Predominantly, friction in this lubrication state arises due to the shear force existing between the solid surfaces and the fluid film, with the viscosity of the fluid film playing a pivotal role in determining friction. The utilization of electromagnetically responsive fluid lubricants under electric or magnetic fields can facilitate reversible control of the interfacial friction [24–27]. This control is achieved through alterations in the fluid's viscosity, which are induced by structural transformations of fluid molecules under the influence of electromagnetism. In the state of boundary lubrication, the solid surface is covered with a boundary lubrication film of single or multiple molecular thicknesses, which is either physically or chemically adhered. The external load is supported either by the boundary lubrication film itself and the distributed asperity peaks that penetrate the film (on a rough surface) or solely by the boundary lubrication film (on an atomically smooth surface) [21,28]. For rough surfaces, the interfacial friction is primarily governed by the shear stress of the boundary lubrication film and the asperity peak surfaces. It is important to note that asperity peaks, being inherently solid materials, generate significant shear stress. Conversely, the boundary lubrication film, characterized by its low modulus or low surface energy, produces a relatively small shear stress. The formation and performance of the boundary lubrication film are integral to potential-controlled boundary lubrication. This utilization of potential to control boundary lubrication is also referred to as potential-controlled friction. In practical engineering scenarios, mixed lubrication is frequently observed during shifts in operational conditions. This form of lubrication is distinguished by its unique combination of both boundary and fluid lubrication characteristics.

In the realm of friction interfaces, potentials can either augment or diminish shear stress through the creation or dissolution of boundary lubrication films. These films, within a potential environment, may comprise gas films [29], organic molecular films [20,30,31], water and hydrated ionic films [32–34], and oxide and compound films [35,36], among others. While previous reviews have explored potential-controlled friction [9,10,37], a comprehensive summary of the formation and transformation of boundary lubrication films under electrical fields/potentials remains absent. In 2020, Spikes [38] investigated the influence of electrochemical potential on friction and wear behavior within the lubricating contact zone. However, their concentration was primarily on the system design of potential control, with a particular emphasis on the potential control of friction behavior in organic liquid lubricants. This paper provides a comprehensive summary of potential-controlled friction, especially the formation and transformation of boundary lubrication films under electrical fields/potentials. This is a crucial mechanism underpinning potential-controlled friction. Initially, we introduce two fundamental methods of potential control. Subsequently, we provide an extensive summary of the research advancements in potential-controlled friction over recent decades. We also detail the formation mechanism of boundary lubricating films, categorizing them according to potential-induced surface redox reactions, interface physical adsorption, and interface molecular structure transformations. Subsequently, we collate the predominant factors influencing electronic control friction. Lastly, we reflect upon the possible contributions and hurdles faced by tribotronics within the landscape of industrial production. A comprehensive depiction of the framework is

provided in Figure 2. This review aims to spark inspiration amongst scholars immersed in tribology research and serve as a resource for those involved in manufacturing processes.

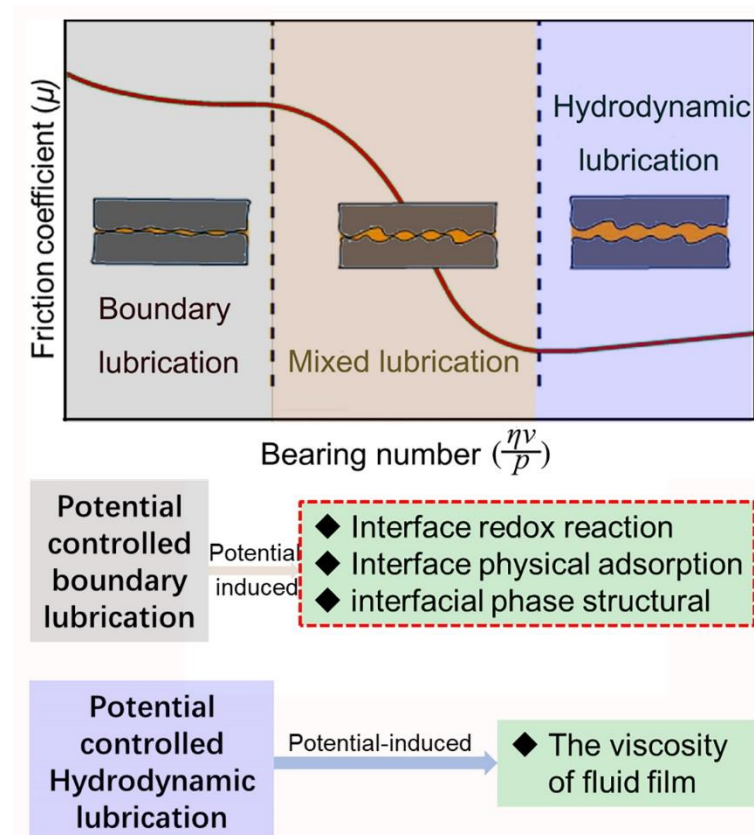


Figure 1. The Stribeck curve delineates three distinct lubrication regimes, with the interface effects of potential significantly influencing both boundary and hydrodynamic lubrication.

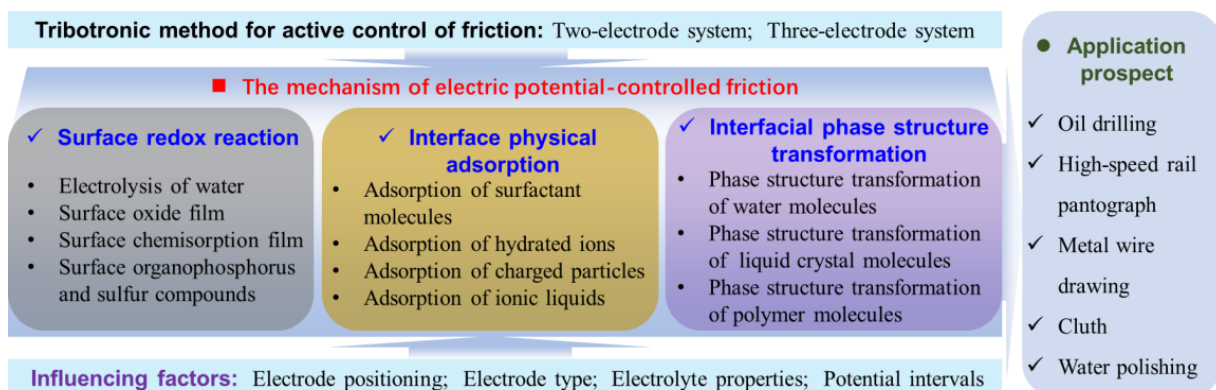


Figure 2. The illustration presents the framework of this review, encompassing the tribotronic method, its underlying mechanism, associated influencing factors, and potential applications.

2. Two- and Three-Electrode Systems

Potential-controlled friction necessitates the use of potential/electric fields to alter interactions between interfaces. Potential-controlled friction systems that exploit potential/electric fields encompass two-electrode and three-electrode systems. A typical two-electrode friction system is illustrated in Figure 3a, where the entire friction pair is immersed in a solution, with the two friction surfaces acting as the working electrode and the counter electrode, respectively. The frictional performance of the interface is regulated by applying voltage across these surfaces. This control method is characterized by its simplicity and

efficiency, particularly demonstrating excellent regulation effects in oil-based lubricants with poor conductivity. This approach has been widely employed by numerous researchers in the early stages of study. In the two-electrode system depicted in Figure 3b, the lower friction pair serves as the working electrode, with the auxiliary electrode acting as the counter electrode. The frictional properties of the interface can be controlled by adjusting the relative voltage between the working and counter electrodes. In this control system, the upper friction pair, which can be composed of non-conductive materials such as ceramics or polymers, does not directly connect with the electrodes. Recent research suggests that integrating this electronic control system with a quartz crystal microbalance offers a powerful tool for investigating the triboelectronics of nanoparticle suspensions and ionic liquids [39]. Employing this approach to assess the efficacy and responsiveness of a range of materials sensitive to electric fields may fast-track advancements in the realm of electric potential-controlled friction [40]. In the control system of Figure 3c, neither the upper nor lower friction pairs serve as electrode materials. The gradient distribution of frictional attributes can be attained by regulating the spatial distribution of interfacial reactions; this regulation is accomplished through intricate adjustments of the current within the solution [41]. Despite its simplicity, the two-electrode system has notable shortcomings. Firstly, the precise definition of the true potential on the electrode surface poses a challenge. Even in the absence of applied potential, the electrode potential relative to the standard hydrogen electrode varies amongst different metal electrodes due to their distinct electron gain and loss capabilities. In a two-electrode system, the absence of a reference potential means that the applied potential is merely the voltage difference between the two electrodes, making it difficult to accurately determine the true potential on the electrode surface. Furthermore, the lubricating film situated at the friction pair interface contributes to a voltage drop. As the friction interface undergoes movement, fluctuations in the lubricating film's thickness cause the interface voltage difference to destabilize, a phenomenon that is challenging to precisely define. This inability to accurately determine the interfacial potential impedes the quantitative study of interfacial reactions. Secondly, the lubricating film between the friction interfaces, typically only several to a dozen nanometers thick, provides limited electrical impedance. A marginally higher voltage can easily breach the lubricating film's barrier, leading to an interface short circuit. Alternatively, during the friction process, the lubricating film may be compromised by the scraping effect of minuscule peaks, resulting in direct interface contact and the formation of a short circuit. Such short-circuited interfaces disrupt the equilibrium reaction between the original electrode and lubricant molecules, leading to suboptimal potential regulation.

In contrast to the two-electrode system, the three-electrode configuration offers superior potential precision and stability, making it particularly advantageous for the design of devices and equipment related to electronic friction control. As depicted in Figure 3d–f, this three-electrode system comprises a working electrode, a reference electrode, and a counter electrode. The current flows between the working and counter electrodes, while the reference electrode maintains a reference potential. The potential at the working electrode's surface is modulated about this reference potential, thus rendering the surface potential of the working electrode as the actual potential. This system design aids in the precise adjustment of interface potential, thereby facilitating a more accurate study of interfacial triboelectrochemical reactions. In Figure 3d, the lower friction pair serves as the working electrode, while the upper friction pair remains uninvolved in the electrochemical reaction, and can be composed of non-conductive materials such as ceramics or polymers. Interface friction is regulated by controlling the potential at the friction pair's surface. Figure 3e portrays a scenario where both the upper and lower friction pairs function as working electrodes concurrently, resulting in identical potentials and similar electrochemical reactions on both surfaces. In Figure 3f, neither the upper nor the lower friction pairs are directly connected to any electrode, allowing for the possibility of the friction pair materials being entirely insulating. By fine-tuning the relative position of the friction interface and the electrode system, it is possible to influence the distribution of the boundary lubricating film at

the interface. Consequently, even though the frictional pair does not engage in the electrode reaction, this tuning allows its friction performance to be potential-modulated [42].

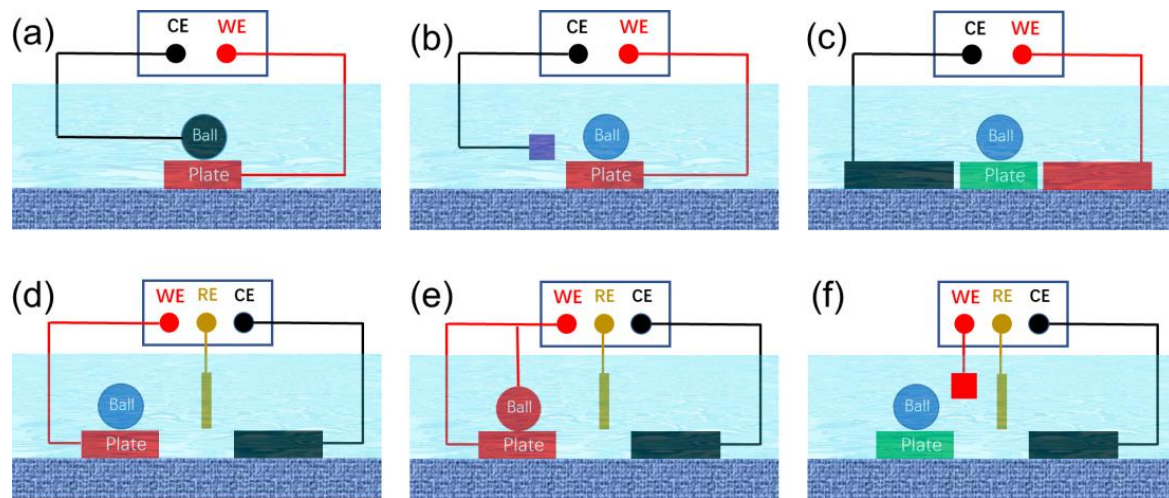


Figure 3. Schematic of a series of electric potential-controlled friction devices (a) A two-electrode control system where the lower friction pair serves as the working electrode while the upper friction pair functions as the counter electrode. (b) In a two-electrode control system where the lower friction pair is employed as the working electrode an auxiliary electrode acts as the counter electrode. (c) A two-electrode control system where the upper and lower friction pairs are not directly linked to the electrode system. (d) A three-electrode control system where the friction pair serves as the working electrode and an auxiliary electrode functions as the counter electrode. (e) A three-electrode control system where both upper and lower friction pairs simultaneously operate as working electrodes. (f) A three-electrode control system in which the upper and lower friction pairs are not directly connected to the electrode system.

In practical lubrication systems, lubricants adopting hydrocarbon-based ingredients typically exhibit limited conductivity. A more suitable approach appears to involve applying a substantial DC voltage directly onto the friction pair surface using a two-electrode system rather than a three-electrode system. Introducing a supporting electrolyte or leveraging a microelectrode can effectively counteract the poor conductivity of the lubricant, though this strategy is not without drawbacks [43,44]. The competitive adsorption between the supporting electrolyte and the lubricant additive on the electrode surface may compromise the lubricant's performance [38]. The three-electrode system, especially one based on microelectrodes, imposes stringent environmental stipulations, and the spatial relationship between the friction interface and the electrodes could culminate in uneven lubrication performance at the interface boundary [41]. Such conditions constrict the performance tuning capabilities of the three-electrode system within the friction interface of larger equipment. Yet, the precision inherent in the potential of a three-electrode system, along with the convenient quantitative analysis of the electrode process, can prove beneficial for designing compact, high-precision electronic friction transmission systems. Such systems stand to make accurate and swift friction transmission a reality.

3. The Mechanism of Potential-Controlled Friction

3.1. Interface Redox Reaction

In electrochemical environments, atoms, molecules, and ions near the electrode interface are stimulated by the externally applied electric field/potential, leading to electron transfer among them. This induces the formation of a boundary film due to the irreversible redox reactions at the interface, altering interfacial frictional behavior. Based on the type of boundary lubrication film, these interfacial redox reactions can be categorized into

electrolysis of water, formation of surface oxides, formation of surface chemisorbed films, formation of surface organic phosphorus and sulfur compounds, and so on.

3.1.1. Electrolysis of Water

In 1874, Edison demonstrated that applying an electrical potential difference between two surfaces can alter their frictional behavior [45]. He investigated various materials and discovered that electric fields can either decrease or increase friction depending on the material [38]. This method of electric field modulation is highly practical and holds significant implications for active friction control. However, Edison did not delve further into the mechanism of potential-controlled friction, merely suggesting that friction reduction might result from hydrogen generated by electrolytic water-reducing metal oxide formation [45]. Subsequent studies with inert metal platinum did not observe a similar phenomenon [46]. Bowden and Young examined the potential-controlled friction behavior between platinum wires and platinum cylinders in dilute sulfuric acid [29]. They observed higher friction at mid-potential and lower friction at negative and high potentials. They proposed that the reduced friction resulted from the generation of single-molecule films of hydrogen and oxygen at corresponding potential intervals, but this “gas film” hypothesis lacked direct evidence.

3.1.2. Surface Oxide Film

In the pursuit of understanding potential-controlled friction, early research predominantly employed platinum electrodes as friction materials due to their inert and oxidation-resistant properties. However, engineering metal materials are prone to electrochemical oxidation at high potentials, consequently altering interfacial friction behavior. In 1988, Pearson et al. [47] discovered that suitable overpotentials could foster oxide film formation on metal surfaces, specifically nickel and alloy steel in NaClO_4 solution. However, the friction effect can disrupt the oxide film and expedite wear. This finding seemingly suggests that increased potential exacerbates wear, but the wear rate fluctuates depending on the oxide film type. In 1994, Zhu et al. [36] investigated the impact of electrode potential on friction and wear behavior between iron/iron friction pairs in a 0.02 M Na_2SO_4 solution. Employing cyclic voltammetry, AC impedance spectroscopy, and infrared spectroscopy, they analyzed the chemical properties of the metal surface film. As potential increased, Fe_3O_4 on the electrode surface gradually transformed into FeOOH , forming a compact and hard δ - FeOOH layer at sufficiently high potentials. Consequently, the COF decreased progressively before a significant drop, while the wear rate initially increased and then decreased. This phenomenon of varying frictional properties due to oxide film differences is widespread. For instance, Kautek et al. [48] examined the frictional behavior of silver/silver friction pairs in alkaline aqueous solutions using lateral force microscopy. They observed a sharp decline in the COF as excessive potential generated silver oxide on the electrode surface. Conversely, Labuda et al. [49] found that gold oxide formation increased the COF, while Liu et al. [50] reported a similar increase in the COF due to copper oxide formed on the surface through friction and electrochemical assistance. These findings demonstrate the direct relationship between surface oxide film and frictional wear behavior. By modulating the potential to control the surface oxide film’s nature, active regulation of frictional wear behavior can be achieved.

3.1.3. Surface Chemisorption Film

In electrolyte solutions containing surfactant molecules, excessively high or low potentials can trigger chemical reactions between surfactant molecules and metal ions on the electrode surface, resulting in the formation of a chemically reactive film. These organic molecular films can substantially enhance the resistance of friction and wear properties. For instance, Zhu et al. [36] demonstrated a significant reduction in interface friction by forming an iron octanoate film on an iron surface through potential elevation. In 1993, Brandon et al. [51] identified three distinct frictional wear zones while investigating the

frictional behavior between mild steels in an alkaline solution containing octanoic acid under electrochemical conditions: high friction/high wear at negative potentials, low friction/high wear at intermediate potentials, and low friction/low wear at positive potentials. They proposed that direct metal contact at cathodic potentials results in high friction and adhesive wear, while the formation of a single molecular layer of octanoic acid on the metal surface at minor cathodic potentials reduces friction. However, this protective film can be disrupted by friction, exacerbating metal corrosion and increasing wear rates. As the potential rises, a more stable film eventually forms, characterized by a “carpet” structure of closely and vertically arranged octanoic acid species in a thicker double or multi-layered configuration. This stable film prevents the exposure of new metal surfaces during friction, leading to significantly reduced corrosive wear. To further evaluate the phenomenon described by Brandon et al. and assess the feasibility of using the adsorption of electroactive species to control friction, Ismail et al. [52] conducted a comparative study on the effects of potential-controlled friction in aqueous solutions of octanoic acid and NaOH. Their findings revealed that positive potentials reduced friction in octanoic acid solutions due to the formation of a chemically reactive iron octanoate film. Conversely, NaOH exhibited a corrosive effect on the metal surface, and the positive potential accelerated corrosion, resulting in increased wear. The authors suggested that potential-controlled friction could be a valuable industrial technique for regulating friction by selecting either cathodic or anodic overpotential.

In 1997, Su and colleagues [53,54] employed potentiometric assistance to generate chemically reactive films, aiming to augment the boundary lubrication performance of copper wire during the drawing process. The researchers utilized oil-in-water (O/W) emulsion lubricants containing fatty acids, in conjunction with an auxiliary applied potential, to bolster the boundary lubrication properties of the copper wires. Their findings revealed that the formation of a fatty acid chemisorption film was contingent upon the prior development of copper oxide on the surface. Furthermore, this chemisorption film was demonstrated to provide effective boundary lubrication. Notably, the application of a positive potential expedited the formation of copper oxide, ensuring the efficacy of this approach in the wire drawing process.

3.1.4. Surface Organophosphorus and Sulfur Compounds

Early investigations into potential-controlled friction predominantly focused on water-based electrolyte solutions, owing to their exceptional electrical conductivity. However, oil-based lubricants are more prevalent in practical applications, where their low electrical conductivity poses challenges in modulating friction using voltage or potential. By employing microelectrodes and supported electrolytes, the electrical conductivity of lubricants can be effectively enhanced, paving the way for research and development in electrically controlled friction within oil-based lubrication systems [43,44]. The achievement of the potential active control of friction in oil-based lubricants primarily relies on physical adsorption [11,55] and chemical reactions [56–58]. A detailed description of the additive physisorption mechanism at the interface will be provided in a subsequent section.

The formation of a friction film with low hardness and elasticity at the interface enhances boundary lubrication performance through the frictional chemical reaction between the additive and the interface [56,59]. Currently, potential-regulating additives for oil-based systems primarily consist of organic compounds containing phosphorus and sulfur elements, such as organic sulfates [11,12,43], zinc dialkyl dithiophosphate (ZDDP) [35,43,60], and Bis(2,3-dichlorophenyl) disulfide phosphate (DBDS) [39]. In 1989 and 1991, Wang and Tung et al. [61–63] introduced ZDDP into a mineral base oil, forming a friction film on cast iron surfaces using an electrochemical control method. However, the high resistance of the mineral base oil postponed the emergence of electrochemical reaction characteristics until several hours after sliding friction initiation. In 2002 and 2007, Xu and Spikes et al. [60,64] incorporated ZDDP as an additive into the more polar diethyl sebacate (DEHS) base lubricant. To further enhance the lubricant’s electrical conductivity, tetradecylammonium

borate (TDATPhFB) was added as a supporting electrolyte. Friction experiment results revealed that electrochemical reactions accelerated the formation of the friction reaction film, reducing the running-in time from tens of minutes at open circuit potential to just a few minutes at a 1.5 V potential. This evidence indicates that electric fields/potentials assist additives in hastening the development of a friction reaction film at the friction interface, thereby promoting a rapid transition to a stable boundary lubrication state.

While widely employed, sulfur and phosphorus additives pose environmental risks and can damage reaction devices such as catalytic converters in automotive engines [35]. The application of electric fields/potentials offers a boundary lubrication effect akin to high-concentration additives while reducing additive content. For instance, Cao et al. [35] investigated the boundary lubrication properties of ZrO₂ balls and AISI 52100 steel sheets under varying potentials in a Propylene carbonate (PC)/Diethyl succinate (DES) mixture with different ZDDP concentrations. They observed that increasing ZDDP concentration enhanced the interfacial boundary lubrication performance, reducing friction coefficient and wear. At a lower ZDDP concentration (2.0% wt), they found that the potential could augment the boundary lubrication performance, with the friction coefficient and wear rate decreasing as the potential increased, as depicted in Figure 4. The thickness of the ZDDP boundary lubrication film at a positive potential (+0.42 V vs. Ag/AgCl) was 30% greater than that at open potential (OCP). The primary chemical components of the ZDDP lubrication film were Fe/Zn phosphate and Fe/Zn sulfide. The authors posited that the applied potential heightened the adsorption capacity of the ZDDP additive at the interface and reduced the activation energy of the interfacial chemical reaction. A recent study by Liu et al. [58] also observed this phenomenon of the potential-assisted formation of thicker friction reaction films. In a DES suspension containing MoS₂, a two-electrode system was employed to investigate the boundary lubrication film at the copper-metal friction interface. It was observed that the application of a +20 V DC voltage resulted in a significantly thicker lubrication film compared to a scenario with no potential applied. The lubrication film comprised Cu₂O-doped MoS₂/MoO_x friction reaction film. This relatively thick and loose friction reaction film played a crucial role in decreasing shear. In a subsequent study, Liu et al. [57] investigated the tribological properties of a bearing steel/ZrO₂ friction pair immersed in PAO oil, which was notably devoid of phosphorus and sulfur-based organic molybdenum additives. They discovered that the formation of a MoO_x friction film on the bearing steel surface significantly augments the lubrication efficacy of the oil. Moreover, the incorporation of voltage assistance serves to further amplify the lubricant's performance.

3.2. Interface Physical Adsorption

In the above research, interfacial redox reactions complicate the electrode process, hindering a precise understanding of potential-controlled friction mechanisms and limiting its applicability in intelligent equipment due to irreversible electrode processes. Consequently, researchers restrict the electrochemical potential to a narrow range, preventing severe redox reactions at the electrode interface. Within this potential range, friction behavior is primarily influenced by the adsorption and desorption of polar particles at the interface. These adsorbed polar particles form a boundary lubrication film, enhancing friction and wear performance. Upon desorption, the lubrication film ceases to exist, leading to reduced friction and wear performance [65,66]. Depending on particle types, the adsorption and desorption mechanisms can be categorized into surfactant molecules, hydrated ions, charged particles, and ionic liquids.

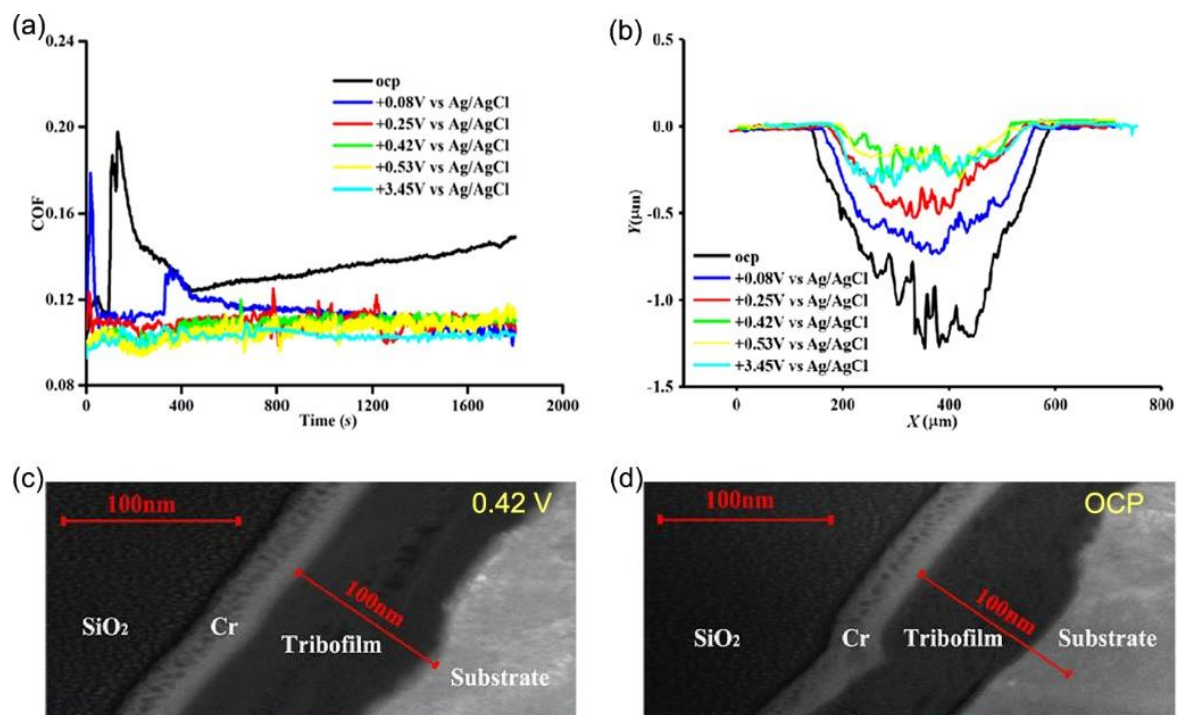


Figure 4. COF, cross-sectional profiles of wear scar, and microscopic morphology of friction reaction films under different potentials. (a) Evolution of COF over time under various potentials, (b) Profile lines of wear scar interfaces under different potentials, (c) TEM morphology of the friction interface at +0.42 V (vs. Ag/AgCl), (d) TEM morphology of the friction interface under open circuit potential. Reprinted from [35], with permission from Elsevier.

3.2.1. Adsorption of Surfactant Molecules

In 1992, Brandon et al. [67] investigated the variations in friction behavior between iron and low-carbon steel under the influence of electrochemical potential in an aqueous solution of octanoic acid (pH 9.2). They discovered that when the potential exceeded the zero charge potential, a caprylic acid lubricating film formed on the electrode surface, leading to a reduced static friction coefficient due to the electrostatic interaction between iron and negatively charged caprylic acid ions. Conversely, when the potential was below the zero charge potential, the lubricating film's formation was hindered, resulting in a significant increase in the static friction coefficient. Furthermore, the reversibility of octanoic acid adsorption was confirmed through cyclic potential measurements. The findings revealed that both the friction coefficient and the hysteresis of scanning capacitance fluctuated during the potential cycle yet returned to their initial values upon the completion of the negative scan, signifying the desorption of the caprylic acid lubricating film.

Since 2009, the research team at Tsinghua University has extensively investigated friction behavior influenced by the adsorption and desorption of surfactant molecules. He et al. [66] initially examined the impact of sodium dodecyl sulfate (SDS) and NaCl concentrations on the friction coefficient's potential response time. They discovered that NaCl concentrations below 50 mM had no significant effect on response time, but concentrations exceeding 500 mM markedly increased the potential response time. For practical applications, NaCl concentrations should be maintained below 10 mM. Subsequently, the researchers applied a dynamic waveform potential to the electrode surface, [68] demonstrating that real-time friction coefficient responses to potential waveforms could be achieved as long as the potential frequency remained below the critical frequency. Within this critical frequency range, lower frequencies resulted in better synchronization between the friction coefficient and potential waveform. To further corroborate the influence of surfactant adsorption and desorption on friction performance, the team characterized the surface morphology of a metal electrode in a 1 mM SDS aqueous solution [12]. They observed that

at positive potentials, surfactants adsorbed onto the electrode surface in a striped pattern, leading to a low friction coefficient. Conversely, at negative potentials, surfactants desorbed from the electrode surface, causing the friction coefficient to increase to levels comparable to those in pure aqueous solutions (see Figure 5). In 2014, Yang et al. [11] demonstrated the extension of potential-controlled friction effects to non-aqueous solutions, achieving reversible regulation of friction behavior between ZrO₂ ball/stainless steel friction pairs in propylene carbonate (PC) solutions containing sodium dodecyl sulfate (SDS) molecules. At a potential of +1.5 V (vs. Ag/AgCl), the interfacial COF remains low due to the adsorption film of SDS molecules. However, when the potential is adjusted to −1.5 V (vs. Ag/AgCl), SDS molecules desorb from the surface, increasing the friction coefficient. Upon returning to +1.5 V, the friction coefficient reverts to its lower state. Later, Zhang et al. [69] systematically investigated the adsorption characteristics of SDS molecules on metal surfaces, discovering that increasing SDS concentration alters the adsorption structure from a monolayer film to a semi-micelle structure. The addition of NaClO₄ significantly reduces the micelle concentration of SDS molecules. Notably, Zhang et al. [41] designed a bipolar electrode system, revealing a substantial spatial distribution effect on the friction coefficient of the electrode surface in SDS aqueous solutions (as depicted in Figure 6). The spatial distribution of the COF corresponds to the adsorption amount of SDS molecules on the electrode surface at various positions. This gradient control technology for surface COFs holds promise for applications in intelligent equipment. Recently, Gao et al. [70] achieved an ultra-low COF between gold electrode/silica sphere friction pairs under negative potential in cetyltrimethylammonium bromide (C₁₆TAB) solutions using electrochemical atomic force microscopy (AFM). This low COF results from the adsorption of C₁₆TAB molecular micelles at the interface, with the hydration layer of the micelles providing exceptionally low shear strength. Conversely, at positive potentials, the desorption of C₁₆TAB leads to a significant increase in the friction coefficient.

In the investigation of tribological property regulation through potential-controlled adsorption and desorption of surfactant molecules, the friction pairs typically involve at least one metallic component. Recently, Liu et al. [42] devised a novel friction system to achieve reversible control of the friction coefficient between an Al₂O₃ disc and a ZrO₂ ball in a solution containing SDS and NaCl (Illustrated in Figure 7). They introduced an indirect adsorption–desorption model, which posits that, despite the non-conductive nature of the friction pair, variations in the electrical properties of the metal ball holder for fixing ceramic balls influence the local concentration of surfactants and ions with distinct electrical characteristics. Consequently, this indirectly impacts the adsorption and desorption behavior of surfactants and ions within the contact region, resulting in potential-dependent alterations in the friction coefficient.

3.2.2. Adsorption of Surface Hydrated Ions

Water molecules, although neutral, exhibit substantial dipole moments. In aqueous solutions, these molecules tightly associate with charged or amphoteric ions, forming hydrated layers [65,71]. Research has demonstrated the effective load-bearing and lubricating properties of metal cation hydration layers [72–74]. By modulating the adsorption and desorption of hydrated ions on electrode surfaces, significant alterations in the tribological characteristics between the electrode and contact substrate can be achieved. Gao et al. [75] reported a reversible shift in the COF between graphite electrodes and SiO₂ microspheres in a Phosphate-Buffered Saline (PBS) solution, driven by potential changes. At positive potentials, enhanced interfacial interactions occurred due to electrostatic and hydrogen bonding reactions between negatively charged hydrated ions adsorbed on the graphite electrode surface and positively charged hydrated ions adsorbed on the SiO₂ microsphere surface, resulting in increased friction. Conversely, at negative potentials, the adsorption of positively charged hydrated ions between both surfaces led to low shear forces and, consequently, reduced friction coefficients. Tivony et al. [32] examined frictional energy dissipation between gold electrodes and mica sheets at varying potentials in LiClO₄ solutions.

They found that at negative potentials, the low shear stress between the gold electrode and hydrated cations accumulated at the mica interface resulted in minimal energy dissipation. At positive potentials, hydrated ions were expelled from the interface between the electrode and mica sheet, causing direct contact between the rough peaks of both surfaces and substantial frictional energy loss, as depicted in Figure 8. Nonetheless, the mechanism underlying high frictional energy dissipation at positive potentials on gold surfaces remains a subject of debate. Experimental results from a surface force apparatus (SFG) and AFM indicate that under positive potentials in the electrolyte, a viscous ice-like water layer forms on the gold surface [76–79]. Pashazanusi and Li et al. [33,34,80–82] proposed that strong hydrogen bonding between this ice-like water layer and the polar friction materials accounts for the high friction. Thus, the tribological mechanism of potential modulation on gold surfaces in salt solutions warrants further investigation.

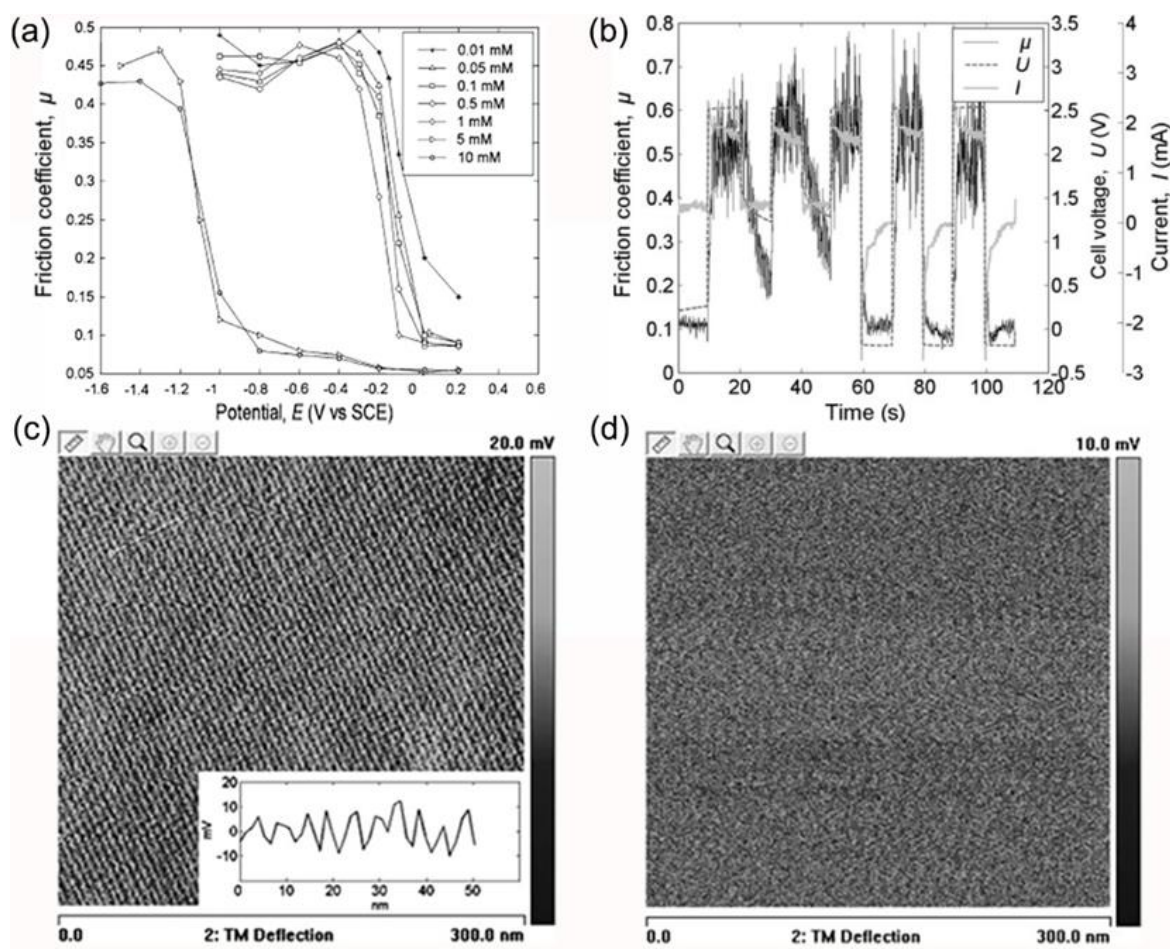


Figure 5. Influence of electrode potential on COF and surface morphology under varying SDS concentrations. (a) Correlation between COF and electrode potential across distinct SDS solution concentrations. (b) Variation of COF under multiple times and different step voltages. (c) Stripe-like adsorption pattern of SDS molecules on the electrode surface at open circuit potential (0.03 V vs. SCE) in 1 mM SDS solution. (d) Absence of SDS molecule adsorption on the surface at a negative potential (-0.4 V vs. SCE). Reproduced from [12,68], with permission from Springer Nature.

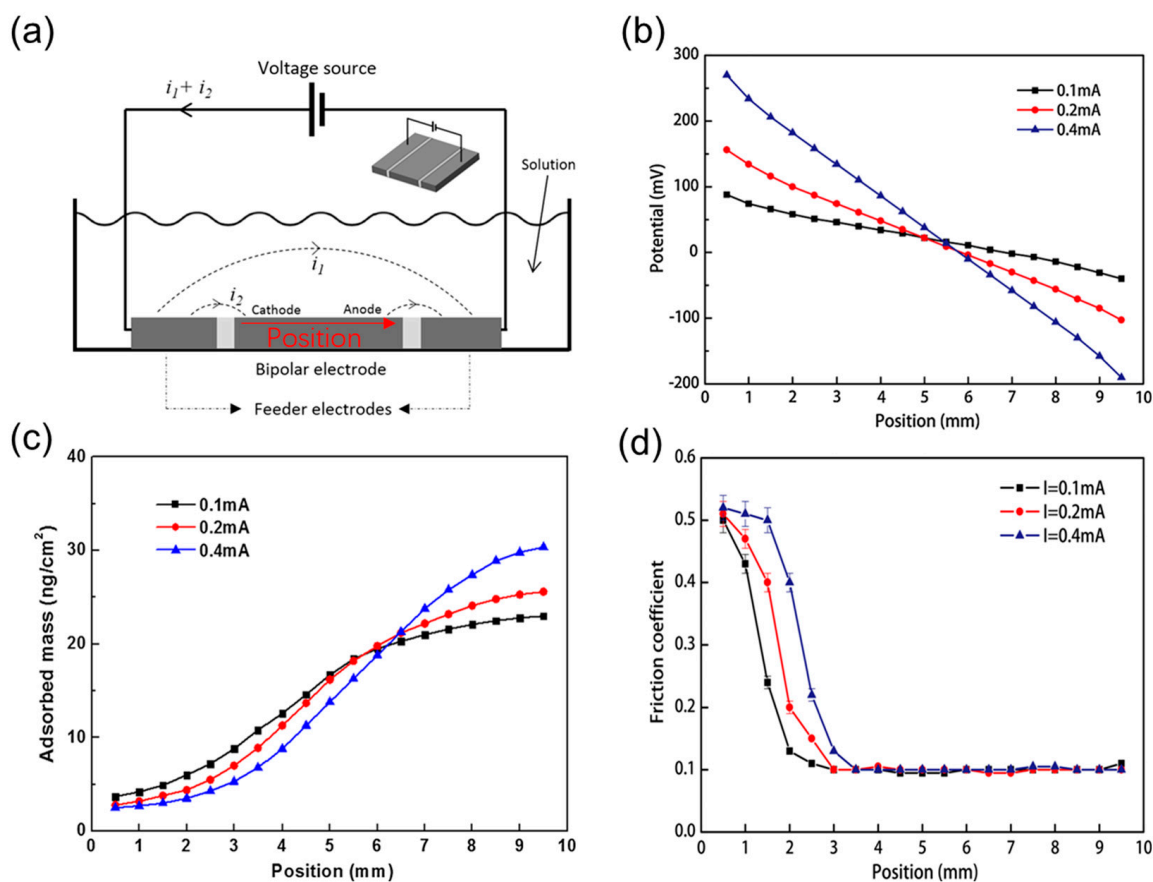


Figure 6. Alterations in tribological properties as a function of electrode surface position. (a) Schematic representation of the bipolar electrode apparatus. (b) Surface potential, (c) adsorption mass of SDS molecules, and (d) interfacial COF at varying locations on the electrode surface. Reproduced from [41], with permission from Springer Nature.

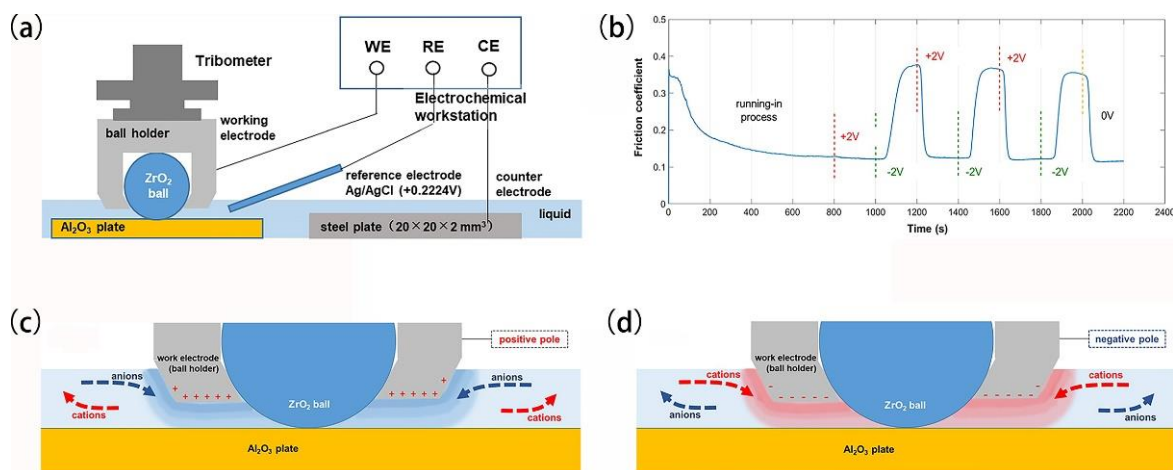


Figure 7. Potential-controlled friction in ceramic tribopairs. (a) Schematic representation of the ceramic tribopair’s electrically modulated friction apparatus, (b) temporal evolution of the COF as a function of applied potential. Illustration of ion dynamics in the vicinity of the interface when the metallic sphere exhibits (c) positive and (d) negative charge states. Reproduced from [42], with permission from Springer Nature.

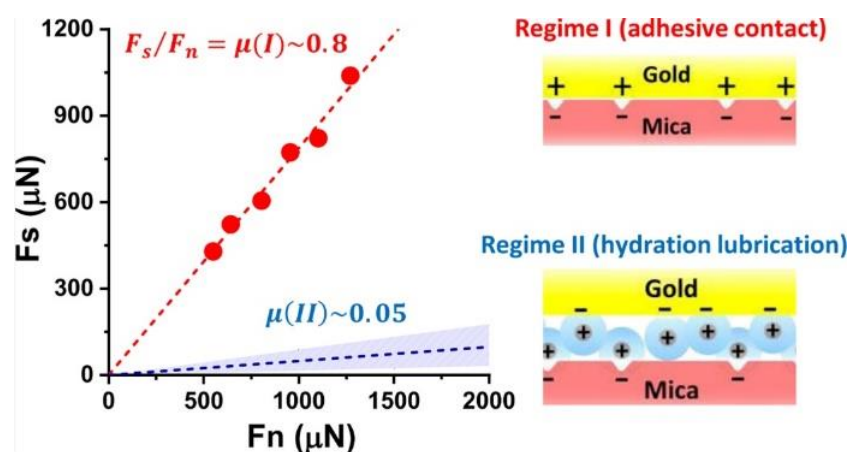


Figure 8. Energy loss and mechanism of friction between gold electrodes and SiO₂ microspheres under different Potentials. Reproduced from [32]. CC BY 4.0.

3.2.3. Adsorption of Charged Particle

Modulating the adsorption and desorption of polar nanoparticles on heterogeneously charged solid surfaces has been found to significantly alter interfacial tribological behavior. Examples include functionalized graphene [83], molybdenum disulfide [58], heat-treated CuS particles [84], functionalized SiO₂ particles, carbon quantum dots [85,86], and charged oxide nanoparticles [87,88]. Typically, potential-induced adsorption of charged nanoparticles on electrode surfaces leads to redox reactions via friction-assisted effects. For instance, fluorinated graphene electrodeposited on stainless steel forms metal-fluorine bonds with the substrate [83], while molybdenum disulfide generates MoS₂/MoO_x under potential influence upon deposition on metal surfaces [58]. However, a recent study by Liu et al. [84] demonstrated that CuS nanoparticles did not undergo chemical reactions with the substrate due to friction. The authors investigated the potential-controlled friction response properties of aminated CuS nanoparticle additives in a diethyl succinate lubricant. The lubricant containing aminated CuS nanoparticles exhibited a pronounced potential-controlled friction effect, characterized by low friction coefficients at negative potentials and high coefficients at positive or zero applied potentials. This behavior can be attributed to the positive electrical properties of the aminated CuS nanoparticle surface, which enables adsorption on the electrode surface at negative potentials, subsequently acting as a boundary lubrication film. However, heat treatment of the aminated nanoparticles led to disordered surface amination molecules, weakening the nanoparticles' electrical properties and diminishing the friction coefficient's responsiveness to potential (see Figure 9). Post-friction characterization of the nanoparticles revealed that CuS nanoparticles did not experience chemical reactions due to friction; rather, the disordered organic molecules on the heat-treated CuS nanoparticle surface were reoriented as a result of friction. In addition, functionalized SiO₂ nanoparticles and carbon quantum dots, poised with a core-shell structure, can generate a boundary-lubricating film on steel surfaces under an electric field, thereby diminishing friction. Intriguingly, applying a counter electric field disrupts this nanoparticle-contained lubricating film, leading to an upsurge in the friction coefficient [85,86]. Significantly, these functionalized nanoparticles readily form chemical bonds with the interface in harsh lubricating environments. Recently, work by C.M. Seed and colleagues sheds light on the friction behavior between a fluid containing charged metal oxide nanoparticles and a flat platinum electrode surface—a study conducted under the influence of an electric field, using a quartz crystal microbalance. The findings illustrate that the inclusion of nanoparticles notably attenuates interface friction between the electrode and the fluid at zero electric field. However, when the electric field propels nanoparticles to adsorb on the platinum electrode surface, interface friction escalates [87,88]. Therefore, it is clear that electric field-driven polar nanoparticles, when deposited on the surface of a friction pair, can form a boundary-lubricating film to suppress friction. Additionally, these nanoparticles

tend to form chemical bonds readily on the surface, facilitated by friction. It is noteworthy that the impact of charged nanoparticles differs across solid–solid and solid–liquid friction regimes.

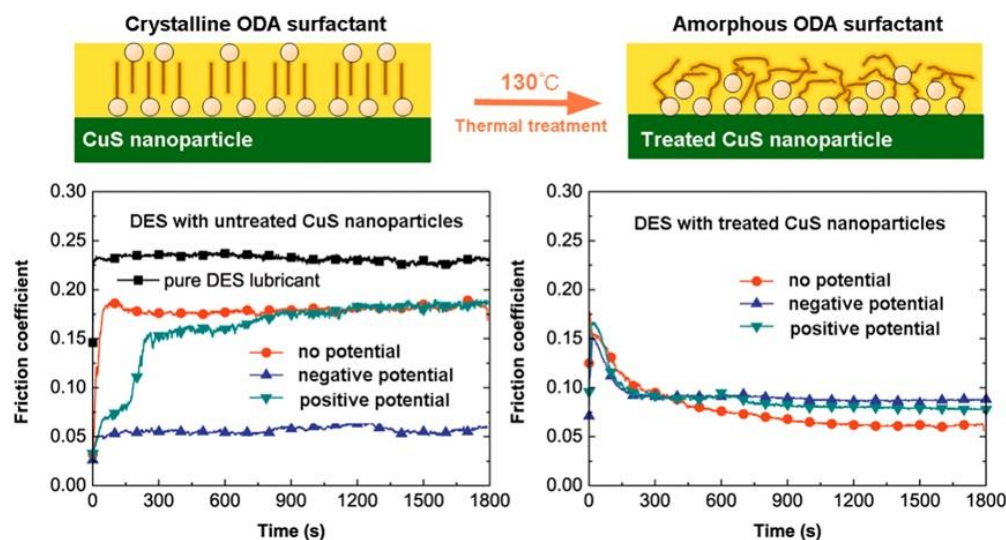


Figure 9. Potential-controlled friction performance of aminated CuS nanoparticles as lubricating additives. This Figure illustrates the orientation of surfactant molecules on the surface of aminated CuS nanoparticles before and after heat treatment at 130 °C. Before heat treatment, an ordered surfactant molecular layer is present, whereas a disordered layer is observed post-treatment. The lower left portion of the Figure displays the friction coefficient of the lubricant containing aminated CuS nanoparticles under varying potentials, demonstrating a significant influence of the applied potential on the COF. Conversely, the lower right portion of the Figure presents the COF of the lubricant with heat-treated aminated CuS nanoparticles at different potentials, revealing minimal changes in the COF as a function of potential. Reprinted with permission from [84], Copyright (2019) American Chemical Society.

3.2.4. Adsorption of Ionic Liquids

Ionic liquids (ILs), characterized as pure salts with melting points below 100 °C [89,90], have garnered attention for their versatile applications in batteries and supercapacitors as electrolytes [91,92] as well as their potential as lubricants [93] due to their high-temperature stability and low vapor pressure. The inherent conductivity of ionic liquids imparts remarkable electrical response properties, enabling the modulation of the adsorption behavior of anions and cations through the potential application, significantly impacting the tribological behavior at interfaces. As depicted in Figure 10a, the 1-butyl-1-methylpyrrolidinium tris(pentafluoroethyl) trifluorophosphate ([Py14] [FAP]) ionic liquid demonstrates a transition from cation enrichment at negative potentials to anion enrichment at positive potentials at the silica colloidal probe and Au(111) interface. This leads to a shift from low friction at negative potentials to high friction at positive potentials [20]. The low friction observed at negative potentials can be attributed to the strong electrostatic binding of cations to the substrate, preventing the ionic liquid from being extruded during friction, and the effective lubrication provided by the alkyl terminus of the lubricant film, which prevents interfacial sticking [20,94,95]. Conversely, the ionic liquid 1-hexyl-3-methylimidazolium tris(pentafluoroethyl)trifluorophosphate ([HMIM] [FAP]) exhibits an opposite potential-controlled frictional behavior between the sharp atomic force probe and the HOPG surface (Figure 10b). The friction force and coefficient are lower at positive potentials compared to negative potentials [96]. At negative potential, cations are enriched on the HOPG surface, forming a flat adsorption film. However, when the atomic force tip traverses the surface, the cations are attracted to the negatively charged tip and reorient to maintain overall electrical neutrality, consuming energy and increasing friction. Under positive potential,

no reorientation of the anion repositioning occurs, and the enriched anion forms a smooth lubricating film, resulting in an ultra-low coefficient of friction and friction [96].

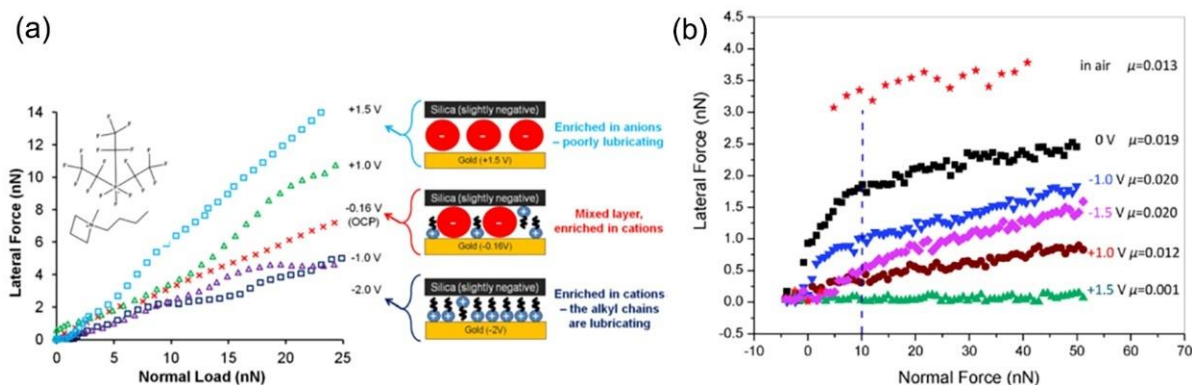


Figure 10. (a) Investigation of frictional behavior and ion adsorption states for silicon spheres and Au(111) substrates under the lubrication of [Py14] [FAP] ionic liquid at varying potentials. Reprinted with permission from [20], copyright (2012) American Physical Society. (b) Analysis of frictional properties between sharp silicon probes and graphite substrates employing [HMIM] [FAP] ionic liquid lubrication across a range of potentials. Reprinted with permission from [96], Copyright 2014, Royal Society of Chemistry.

In a recent study by Li et al. [97], the authors conducted a comparative investigation on the potential-controlled friction behavior of gold and highly oriented pyrolytic graphite (HOPG) electrode surfaces immersed in lithium tetraglyme bis(trifluoromethylsulfonyl)amide (Li(G4)TFSI) ionic liquid. Intriguingly, they discovered that despite employing the same ionic liquid, the two electrode surfaces exhibited contrasting potential-controlled friction phenomena. At negative potentials, the friction magnitudes on both electrode surfaces were found to be similar, suggesting that the adsorbed boundary films on these surfaces exhibit striking resemblances, with both being enriched with Li^+ cations. However, under positive potentials, the hydrophobic interaction between the fluorocarbon anion unit and gold atoms results in an exceedingly weak affinity between the gold electrode and TFSI $^-$ ions. Consequently, the adsorbed films are more prone to being sheared off under high stress, giving rise to rougher sliding surfaces and diminished lubrication properties.

As observed, the potential-controlled friction effect of ionic liquids is influenced not only by the potential but also by variations in electrode properties. Factors such as molecular chain length, concentration, and composition of ionic liquids can significantly impact this effect. For instance, Kong et al. [98] discovered that ionic liquid molecules with shorter chains exhibit a more pronounced potential-controlled friction effect. In contrast, Cooper and Pilkington et al. [99,100] reported a more substantial effect for highly concentrated ionic liquids. Gatti et al. [101] found that utilizing hybrid ionic liquids, comprising long-chain cations and two distinct high charge/mass ratio anions, resulted in a markedly higher magnitude and speed of the potential-controlled friction effect compared to single-type ionic liquids. Consequently, rational adjustment of potential-controlled friction system parameters with ionic liquids facilitates the design of high-precision and rapidly adjustable electro-controlled friction actuators.

3.3. Interfacial Phase Structural Transformation

Under the influence of an external electric field/potential, charged particles often exhibit a certain degree of hysteresis in adsorption and desorption at the electrode interface. This phenomenon poses a challenge to the design of precision electro-control friction devices [31,68,84]. A potentially more effective strategy for creating such devices may involve modulating the in situ orientation and structural arrangement of the interfacial molecular layer in response to the potential/electric fields, thereby enabling the interfacial frictional properties to respond more swiftly [30]. Indeed, Drummond and Li's research [30,33] achieved an

instantaneous friction coefficient response to the potential/electric fields by transforming the interfacial molecular structure. Molecules reported to undergo structural changes in response to potential/electric fields in studies of potential-controlled friction include water, liquid crystal, polymer molecules, etc.

3.3.1. Phase Structure Transformation of Water Molecules

In aqueous solutions, the viscosity of the confined layer at the electrode interface at a specific potential is approximately 10^{5-7} times greater than that of the bulk phase solution [77,78,80]. High-resolution spectroscopy and molecular dynamics investigations have revealed a strong correlation between the increased interfacial viscosity and the ice-like water layer formed by water molecules at the electrode interface [77,79,102]. The friction behavior can be actively modulated by adjusting the electrode surface potential, which in turn alters the structure of the interfacial water layer. Pashazanusi et al. [80] explored the friction behavior between SiO₂ microspheres and gold surfaces using electrochemical atomic force microscopy (EC-AFM). They discovered that friction at a positive potential (+0.6 V vs. Ag) was approximately 35 times greater than that at a negative potential (−0.6 V vs. Ag). This difference occurs because an ice-like water layer forms on the gold surface under positive potential, while the ice-like water layer's structure is disrupted under negative potential, allowing free water molecules to act as boundary lubricants. This interfacial structure transition results in potential-controlled friction behavior. Li et al. [34] observed that under the same experimental conditions, friction and adhesion between hydrophobic polystyrene microspheres and gold electrodes remained unchanged with potential, whereas hydrophilic SiO₂ microspheres exhibited electrically controlled friction phenomena similar to those in Pashazanusi's study. Consequently, they proposed a hydrogen bonding hypothesis between the ice-like water layer and SiO₂ microspheres. Under positive potential, the ice-like water layer on the gold surface forms strong hydrogen bonds with the hydroxyl groups on the SiO₂ microsphere surface, thereby increasing friction. In contrast, the polystyrene microsphere surface lacks hydroxyl groups, and the friction behavior remains unaffected by potential. Li et al. [33] later achieved a rapid reversible transition between superlubricity under a negative potential and high friction under a positive potential using a small load. They analyzed the quantitative relationship between load, adhesion, and friction under a positive potential using friction binomials, revealing that the load-determined friction was minimal. The adhesion and friction between interfaces under a positive potential are primarily attributed to the hydrogen bonding force between the ice-like water layer and the hydroxyl groups on the SiO₂ surface, as illustrated in Figure 11. Recently, Li et al. [82] also identified differences in hydrogen bonding mechanisms between positive microspheres (−NH₃ terminal microspheres) and negative microspheres (−OH and −COOH terminal microspheres) and the ice-like water layer. Negative microspheres directly form hydrogen bonds with the ice-like water layer through surface polar groups, while positive microspheres generate hydrogen bond sets with the ice-like water layer through hydrating anions adsorbed on the surface within their hydration shell.

The studies mentioned above were conducted in salt solutions. Although electrochemical analyses indicated an absence of redox reactions and substantial ion adsorption on the electrode surface within the selected potential range [34,80], it is improbable that ion adsorption effects are entirely negligible. In a collaborative investigation, Pashazanusi and Li et al. [81] discovered that the potential increase induced by friction between a silicon needle tip and a gold electrode surface in NaOH solution was lower than that in NaCl solution. This observation can be attributed to the fact that Cl[−] ions are more disruptive to ice-like water layers compared to OH[−] ions, necessitating a higher potential in NaCl solutions to establish a stable, viscous water layer at the gold interface. Consequently, further research is warranted to elucidate the formation and structure of ionic and ice-like aqueous layers in these systems.

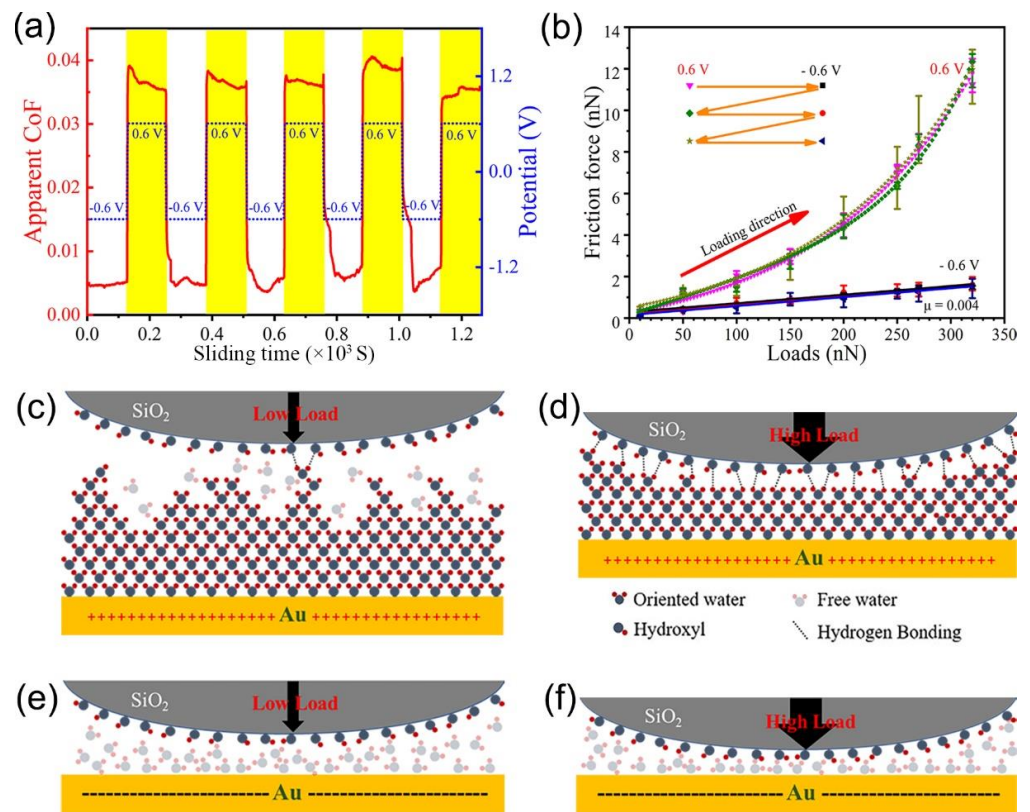


Figure 11. Potential-regulated frictional behavior and mechanisms at the gold electrode interface. (a) Rapid and reversible transitions between superlubricity and high friction states are achieved through potential modulation of the gold electrode surface. (b) Friction-load dependence at positive and negative potentials on the gold electrode surface. At positive potentials, (c) a limited number of hydrogen bonds form at the interface under low-load contact, while (d) an extensive hydrogen bonding network develops under high-load contact. (e,f) Under negative potential, the ordered ice-like structure of water molecules is disrupted, allowing free water molecules to act as boundary lubricants, thereby reducing frictional forces. Reproduced from [33]. CC BY 4.0.

3.3.2. Phase Structure Transformation of Liquid Crystal Molecules

Liquid crystals, with their ordered molecular structures, have proven to be a valuable asset in investigating boundary lubrication mechanisms [103]. Studies have shown that the use of liquid crystals as lubricants or lubricating additives can markedly augment lubrication effects [104,105]. The dielectric anisotropy of liquid crystal molecules allows electric fields to modify their orientation, subsequently modulating the viscosity and lubrication performance of liquid crystal boundary lubrication films [106–110]. In 1994, Kimura et al. [109] investigated the electric lubrication behavior of thermo-induced liquid crystals by applying a DC voltage to a sliding pin and steel ball contact pair. Their findings revealed a COF reduction of approximately 25% when the voltage increased to 30 V. A similar friction reduction was observed when a low-frequency alternating current of less than 1 Hz was applied. In 2015, Manzato et al. [111] utilized molecular dynamics simulations to examine the lubrication performance of nematic liquid crystals under the influence of electric fields. They discovered that electric fields could regulate the orientation of liquid crystal molecules, thereby controlling friction performance. When an in-plane electric field perpendicular to the sliding direction was applied, relative friction increased; conversely, when the field was applied along the sliding direction, friction decreased. In 2017, Gao et al. [103] employed in situ infrared spectroscopy to study the molecular orientation and frictional behavior of nematic liquid crystal 4-n-pentyl-40-cyanobiphenyl (5CB) during friction under electric fields. They found that at low sliding speeds, the liquid crystal molecules, influenced by the electric field, adopted a vertical arrangement, increasing the

liquid crystal viscosity. Consequently, the lubrication film in the contact zone became more stable, significantly improving lubrication performance. However, at high sliding speeds, the electric field weakened the orientation of liquid crystal molecules, resulting in a decreased electric field response-ability for lubrication performance. In summary, the primary mechanism by which electric fields impact the lubrication performance of liquid crystal molecules is by altering their orientation within the contact area, leading to changes in the lubrication film's properties.

3.3.3. Phase Structure Transformation of Interfacial Polymer

Over the past several decades, significant advancements have been made in elucidating the surface forces governing polymer coatings. Research has demonstrated that these coatings offer effective lubrication in solvents, reducing friction by up to two orders of magnitude in comparison to uncoated surfaces. This remarkable reduction in friction can be attributed to the long-range entropic repulsive forces between the polymer coatings, which maintain a limited separation distance between the surfaces [65,112]. Conversely, external stimuli, such as electric fields, can modulate the lubricating properties of polymer coatings by altering the conformation of the polymer chains. Drummond et al. [30] probed the influence of electric potential on the structure of polymer layers on semi-cylindrical surfaces using a surface force apparatus. While the effect of direct current (DC) potential on friction was inconsequential, friction was substantially reduced when the alternating current (AC) potential difference reached 600 Hz. However, this potential effect vanished beyond 600 Hz. Drummond et al. proposed that the swift motion of counterions in the solution, under the influence of AC potential, induced stretching and bending of the polymer chains, thereby eliminating the impact of interpenetration on the coupled surfaces. The potential response effect on friction dissipates when the polymer cannot swiftly adapt to environmental changes. Zeng et al. [113] employed electric fields to manipulate the polymer structure, achieving reversible alterations in friction. They observed that on indium tin oxide (ITO) glass surfaces, the morphology of poly-sodium allyloxy hydroxypropyl sulfonate (poly-AHPS) polymer oscillated between a brush array morphology when stretched at negative potentials and a hill-roll morphology at positive potentials, resulting in two distinct frictional states. The authors concluded that this approach holds promise for the automatic control of friction and has potential applications in automation, intelligent manipulation and actuation, as well as microelectromechanical systems. In a recent study, Li et al. [114] investigated the potential-controlled friction effect in polymer ionic liquids, specifically poly(3-methyl-1-aminopropylimidazolium acrylamide) bis(trifluoromethylsulfonyl)imide (Poly(3MAPIIm)TFSI). They focused on the stretching and compression properties of cationic chains within these polymers to modulate frictional behavior. Under negative potential, a significant enrichment of polycations occurs on the Au(111) surface. This accumulation results in the compression of cation chains due to electrostatic attraction, subsequently increasing the lubricant film's surface roughness. Concurrently, the attractive forces between the AFM probe and the cations in the boundary lubrication layer contribute to an elevation in friction. Conversely, under a positive potential, the quantity of cationic adsorption is reduced due to electrostatic repulsion, thereby providing ample space for the cationic chain to unfurl. Concurrently, the TFSI with better lubrication performance adsorbs on the surface, leading to a reduction in the friction force. The findings suggest that potential-controlled changes in the polymer structure, primarily driven by the extension and compression of the polymer chain, are the main factors influencing friction performance. When the polymer chain within the lubricating film extends, it effectively separates the two friction surfaces and diminishes the interaction force between them. On the other hand, when the polymer chain is bent and compressed, the lubricating film's surface becomes rougher, and the interaction force between the surfaces increases [30,113,114].

3.4. Mechanism Summary

The fundamental principle of potential-controlled friction lies in the potential or electric field-induced alterations in the physical or chemical properties of the friction interface. The potential impact on friction can be categorized into three primary mechanisms. First, the interfacial charge directly participates in the interfacial chemical reactions. Examples include the formation of metal electrode surface oxides or hydroxides at positive potentials, the development of friction-reactive films with low shear modulus and low hardness at the friction interface due to additives containing sulfur or phosphorus, and the creation of chemically reactive adsorption films through surfactant molecules chemically bonding to the interfacial metal. Second, the interface charge does not partake in the reaction, but the potential or electric field prompts the counter-electrode material to accumulate on the electrode surface, forming a physically adsorbed film. Instances of this mechanism include the adsorption films of surfactant molecules, hydrated ions, polar nanoparticles, and ionic liquids. Lastly, the potential or electric field induces structural changes in the interfacial adsorption film. For example, water molecule layers transition between liquid and ice-like states, liquid crystal molecules switch between ordered and disordered configurations and polymer molecular chains alternate between stretched and bent conformations. The formation and structural transformation of the adsorption film at the friction interface lead to variations in interfacial adhesion and shear, ultimately resulting in the phenomenon of electrically controlled friction.

4. Influencing Factors of Electro/Potential-Controlled Friction

In potential-controlled friction systems, the potential serves as the primary factor influencing friction behavior, while variations in the system's composition and parameters dictate the specific potential-controlled friction characteristics. Figure 12 illustrates the dynamic interplay between the modulation of the friction coefficient and potential, as observed in several representative pieces of literature on electronically controlled friction [115]. These studies deploy varied electrode materials, lubricants, and potentials/voltages, rendering a direct comparison of their results challenging. Research has demonstrated that electrode positioning [41], electrode type [81,97], electrolyte properties [42,81], and potential intervals [50] all significantly impact electro-controlled friction behavior.

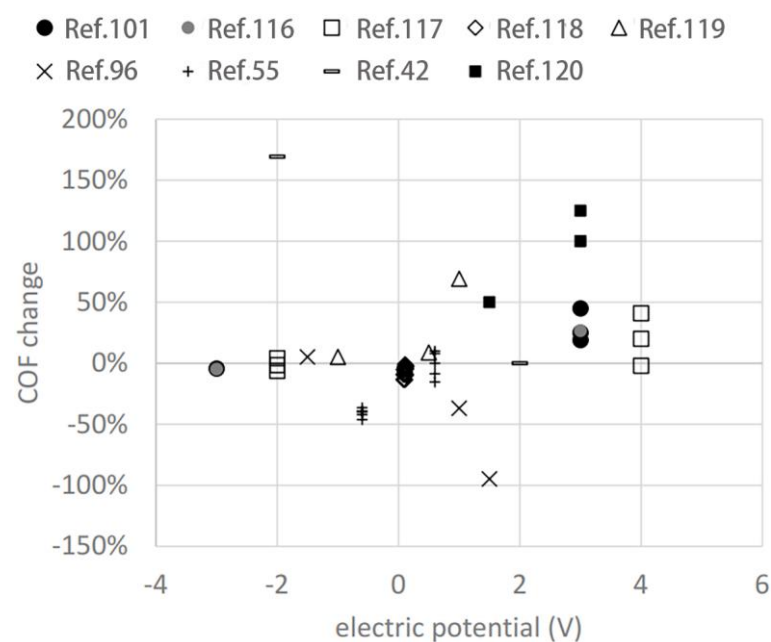


Figure 12. The change in the COF versus electric potential is derived from data presented in some typical papers [42,55,96,101,116–120]. Reproduced from [115]. CC BY 4.0.

In a three-electrode electrochemical system, the counter electrode's relative position to the working electrode or between the counter electrode and the friction region influences the electro-controlled friction behavior on the working electrode surface. When the counter electrode's relative position and the friction region are adjusted so that the friction region falls within the electrode's influence, the potential exhibits a substantial modulating effect on friction performance. Conversely, when the friction region lies far from the electrode's influence, the potential-controlled friction effect is not achieved [41]. In a bipolar electrode system, the rational design enables spatial positioning of the electrode surface potential to control frictional properties at different locations on the electrode surface [121]. Investigations using imaging surface plasmon resonance (ISPR) and ellipsometric polarization spectroscopy have examined this gradient distribution of molecular films. By varying the solution current, the distribution of molecular adsorption with spatial location can be modulated [122], and the adsorbed film can serve as a boundary film. The boundary lubrication effect is closely related to its adsorbed amount and adsorption structure [123]. It is hypothesized that using bipolar electrodes as friction subsets allows the spatial distribution of electric potential to control the friction coefficient distribution with spatial location. Supporting this conjecture, Zhang et al. [41] achieved a gradient distribution of the COF over the spatial position on a bipolar plate. By examining the surface potential and molecular adsorption at different locations on the bipolar plate, a gradient distribution was observed for both surface potential and SDS molecular adsorption, as illustrated in Figure 6. This finding indicates that the potential's gradient distribution caused the SDS molecular adsorption to exhibit a gradient distribution, subsequently leading to a gradient in the COF. The authors propose that this method of controlling the COF variation with electrode position may hold significant implications for metal-forming processes. For instance, in a drawing process, low friction is necessary for the die area to reduce sliding resistance and tensile stress in the cup wall, while high friction is required at the die corners to facilitate metal flow.

The electrode characteristics significantly impact the behavior of potential-controlled friction systems. As previously indicated, despite the utilization of the identical ionic liquid electrolyte, the gold and graphite surfaces exhibit entirely divergent phenomena of potential-controlled friction. This discrepancy is primarily attributed to the variations in the binding strength between the ions and the respective electrode surfaces [97]. Furthermore, when comparing gold electrodes with different surface roughness, the friction coefficient and its shift amplitude are lower for gold electrodes with minimal roughness compared to those with higher roughness [81]. Gold and graphite are considered inert electrodes, as their surfaces are less prone to redox reactions. In contrast, the surfaces of commonly used engineering metal materials are susceptible to corrosion in electrochemical environments. Consequently, friction behavior and interfacial corrosion often interact and influence one another. For instance, stainless steel electrodes exhibit reduced contact pressure between interfaces due to corrosive wear at anodic potentials. Additionally, the oxide film's lubricating properties contribute to a lower friction coefficient at anodic potentials compared to open circuit and cathodic potentials [51,124]. Friction-induced breakage of the interfacial oxide film causes the open circuit potential to shift in the cathodic direction, leading to surface re-passivation and increased corrosion [51,124,125].

The electrolyte's nature has a direct impact on the electrochemical behavior of an electrode surface. Research demonstrates that the electrolyte primarily influences potential-controlled friction behavior by affecting the adsorption layer on the electrode surface. Li et al. [97] investigated the tribological behavior of Au (111) surfaces in ionic liquids through potential control, revealing that Li(G4)TFSI and Li(G4)NO₃ ionic liquids exhibited similar electronically controlled friction behavior. However, the friction coefficient of Li(G4)NO₃ ionic liquid was nearly double that of Li(G4)TFSI ionic liquid at positive potential. This is attributed to the NO₃⁻ ion adsorption layer at positive potential possessing more defects and surface roughness than the fluorocarbon adsorption layer of TFSI⁻. Liu et al. [42] discovered that after adding NaCl to an SDS aqueous solution, the

metal/ceramic friction pair exhibited a faster potential-controlled friction response ability compared to when using the SDS aqueous solution as an electrolyte. This is because NaCl promotes the formation of SDS micelles, accelerating the adsorption and desorption process of SDS molecules on solid surfaces. Pashazanusi et al. [81] examined the potential-controlled friction behavior between gold electrodes and AFM tips in varying concentrations of NaCl solution. They found that high NaCl concentrations could reduce friction under positive potential. This is due to high salt ion concentrations weakening hydrogen bonding between water molecules on the electrode surface and between water molecules and the AFM tip. Simultaneously, their findings also revealed that Cl^- has a stronger ability to inhibit hydrogen bond formation between interfacial water molecules than OH^- , resulting in NaCl electrolytes requiring a higher potential to achieve a stable high-friction state compared to NaOH electrolytes. In conclusion, the electrolyte's type, concentration, and composition can significantly impact electronically controlled friction effects.

In the potential-controlled friction system, friction behavior is modulated by adjusting the applied potential within a specific potential range. The choice of this potential range significantly impacts the system's friction control efficacy and underlying friction mechanisms. With over 20 years of research and development, Meng Yonggang's team at Tsinghua University has gained substantial insights into selecting the appropriate potential range for potential-controlled friction. Figure 13 presents a schematic representation of the electrode reaction process, both with and without friction, at a given temperature. Within a relatively moderate potential range, the electrode interface experiences solely physical alterations, encompassing phenomena such as the adsorption and desorption of anionic and cationic species [75], charged nanoparticles [58,84], surfactant molecules [11,12,68], water molecules [33,34], among others, in addition to phase transitions. Stable reversibility of potential-controlled friction performance is observed within this potential range. However, under a strong electric field (wide potential), the electrode interface experiences irreversible redox reactions [35,50], leading to a lack of stable reversibility in potential-controlled friction performance. Furthermore, in the case of electrode processes influenced by friction, triboelectrochemical processes, such as friction-induced reduction and friction-inhibited reduction, as well as friction-induced oxidation and friction-inhibited oxidation, also come into play (as depicted in Figure 13) [50]. These processes narrow down the range of potential where only physical changes occur.

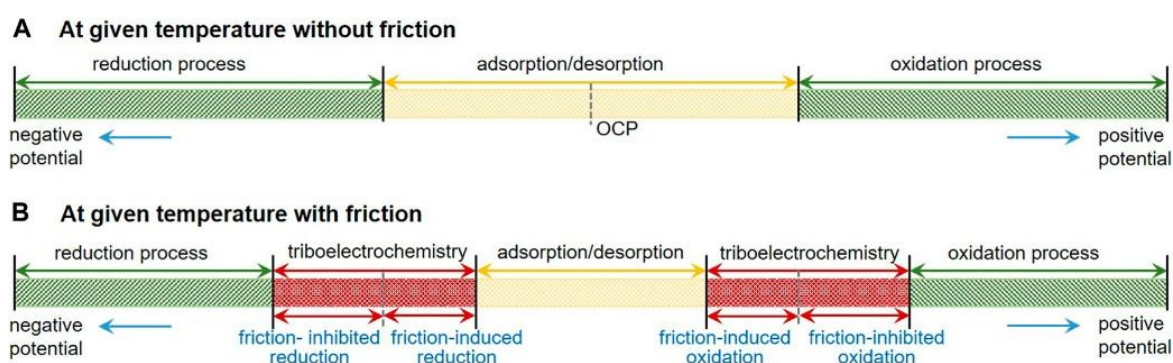


Figure 13. Schematic diagram of the electrode processes at a given temperature without (A) and with (B) friction. Reproduced from [50]. CC BY 4.0.

5. Application Prospect

Potential-controlled friction is a multifaceted triboelectrochemical phenomenon that encompasses electrical, frictional, and chemical interactions in solution. Investigating the performance and underlying mechanisms can offer valuable insights into engineering challenges associated with this phenomenon. By actively controlling friction, it is possible to reduce energy consumption and slow down friction-related failures. For instance, in drilling operations, water-based drilling fluids exhibit high friction coefficients, leading to increased

torque and friction resistance on the drill string, which in turn complicates the drilling process. The application of a cathodic potential can reduce the drill string's friction torque by 50% [126]. Utilizing a magnesium sacrificial anode to connect the drill string achieves a similar effect without the need for an external power source. Electronically controlled friction effectively suppresses differential sticking of the drill string in water-based drilling fluids, thereby enhancing drilling efficiency [52,127]. During adverse weather conditions, such as rain and snow, complex triboelectrochemical reactions occur on the surface of copper alloy pantographs used in high-speed railways. Research indicates that increased relative humidity and the presence of water significantly raise the COF and wear rate of the copper surface. The combined effects of water and current shift the interface wear from mild abrasive wear to severe fatigue wear, accompanied by electrochemical oxidation [128,129]. Studying the triboelectrochemical performance and mechanisms provides a theoretical foundation for optimizing pantograph structures and surfaces. In copper wire drawing processes, emulsion lubricants (oil-in-water) facilitate effective lubrication between the copper wire and the mold. The adsorption of fatty acids in the emulsion on the oxide surface primarily contributes to boundary lubrication and applying a potential can further enhance this effect [54]. Subsequent research revealed that an oxide thickness exceeding 6 nm yields the optimal boundary lubrication effect, with cuprous oxide being the most effective oxide type [53].

The investigation of potential friction phenomena holds not only the theoretical importance of comprehending friction interface processes in depth but also the practical value of active friction control. Traditional lubrication systems can only modulate friction by adjusting the normal load, which makes real-time and online regulation of the COF challenging. In contrast, active control of the COF can be achieved through the application of an electric field or manipulation of the friction pair's surface potential. In designing mechanical devices, the aim is often to amplify beneficial friction while minimizing detrimental friction. For instance, clutches and manipulators require time-dependent control of the COF due to the need for rapid transitioning between sliding and locking during operation. Employing the potential for active control of the COF presents an opportunity to enhance the performance of clutches or manipulators. Hu et al. [130] explored the operational characteristics and friction torque response of a custom-built electronically controlled clutch test rig under an applied electric field. They utilized an aqueous SDS solution as the lubricating fluid, graphite as the auxiliary electrode, and a silicon nitride/brass friction plate as the friction substrate. The findings demonstrate a significant correlation between the applied voltage and the friction torque of the electronically controlled friction clutch. Specifically, an augmentation from 0 V to 20 V in the applied voltage results in a two-fold increase in the friction torque. Moreover, the response time of the friction torque to external voltage alterations is approximately 3 s. These observations suggest promising applications of electronic friction technology in friction transmission devices. Nonetheless, a response time in the range of seconds is markedly prolonged when considering high-end precision equipment. This latency most likely arises due to the temporal needs of boundary lubrication film formation and dissipation. It suggests that electro-control systems that depend on molecular adsorption and desorption for regulating boundary lubrication films might be unfit for precision device tribological transmission or wear damage detection tasks. Investigations have highlighted that by managing the structural transformations of interfacial water and polymer molecules under an electric field, the COF can react instantaneously to changes in the electric/potential field [30,33]. This suggests that leveraging electric/potential fields to modulate the properties of boundary lubrication films may forge an effective tactic for precision equipment development.

As research into potential-controlled friction technology intensifies, its applications have expanded into the realm of precision manufacturing. One notable example is the electric field-assisted chemical mechanical polishing/grinding technique. This approach involves the application of an electric field to the friction subsurface within the grinding/polishing system, enabling control over interfacial friction chemistry. Consequently,

the electric field actively governs the dissolution and removal of interfacial materials, thereby optimizing the efficiency of the polishing/grinding solution [131]. Li et al. [132] conducted a study utilizing electrochemical mechanical polishing (ECMP) with hydrogen peroxide and potassium nitrate as electrolytes and colloidal silica as the polishing medium. They successfully performed electric field-assisted polishing on SiC wafers, demonstrating the potential of this innovative technique. The findings reveal that when currents exceed 20 mA/cm^2 , the resultant polished surface exhibits a rough texture. Conversely, at currents approximating 1 mA/cm^2 , the polished surface demonstrates a smooth finish. Zhai et al. [133] employed a tribological electrochemical polishing (TECP) approach to refine Si_3N_4 surfaces in an aqueous-based medium (Mass fraction:water:sodium nitrite:sodium carbonate:sodium phosphate:borax = 495:1.25:1.25:1.25:1.25). Their findings revealed that applying a forward voltage to the metal disc significantly increased the wear track on the Si_3N_4 surface, while the COF remained constant. Conversely, the application of a reverse voltage led to a substantial reduction in both the COF and the abrasion marks on the Si_3N_4 surface. Through experimental law screening, an optimized grinding process offering high grinding efficiency and superior surface quality was achieved. Recently, Liu et al. [50] proposed that the applied electric field functions analogously to external mechanical forces, thus modulating the reaction energy of chemical reactions in an equivalent manner. Specifically, a positive potential on the sample promotes the mechanochemical process, whereas a negative potential inhibits it. Based on this principle, they demonstrated that applying a positive potential to a Ti plate surface in a PC solution resulted in selective frictional oxidative coloration while reversing the voltage caused the coloration effect to vanish. The authors concluded that this technique holds promising potential in fields such as micro and nano processing, information recording, and surface processing.

6. Conclusions and Perspectives

This review examines the advancements in potential-controlled friction research over recent decades, elucidating the fundamental mechanisms and potential industrial applications of this technology. Potential-controlled friction systems primarily involve two- or three-electrode configurations, with mechanisms categorized into interfacial redox reactions, physical adsorption, and phase structure transformations. A comprehensive understanding of these mechanisms paves the way for designing efficient, intelligent, and high-precision systems with wide-ranging applications in traditional industries, smart equipment, and precision machining. Despite significant progress in the theory and systems of potential-controlled friction, challenges persist in both theoretical and practical aspects.

First, real-time characterization of interfacial reactions during potential-controlled friction remains elusive. Discerning the dynamic reaction process at molecular and atomic scales under the potential influence is crucial for comprehending the nature of potential-controlled friction and the origins of friction itself. In situ transmission electron microscopy (TEM) has enabled the observation of atomic transfer processes in nanotips during dry friction [134]. Extending this approach to investigate nanotip friction in electrochemical environments using TEM presents an intriguing challenge.

Second, the interplay between the molecular architecture of the boundary lubrication film and the microscopic forces at the interface presents a complex landscape. The potential, by influencing the interfacial reactions and molecular structure, modulates the interaction forces between the interfaces. Establishing a quantitative correlation between the interfacial molecular structure and the microscopic forces at the interface could pave the way for a direct, quantitative relationship model between the potential and the friction coefficient within an electrochemical system. The formulation of such a model holds the promise of enabling precise and proactive control over the magnitude of the frictional force.

Thirdly, the development of a friction system capable of real-time, rapid, and reversible transformations is still a work in progress. Existing research demonstrates that although potential-controlled friction technology exhibits promising potential for use in transmission systems, a notable hysteresis in friction performance response to applied potentials has been

observed [130]. This hysteresis poses challenges for designing high-precision friction-based transmission systems. While satisfactory real-time responsiveness has been achieved at the microscopic scale, the limited friction rates and loads employed [33] constrain the broader application of electronically controlled friction technology in transmission systems. Consequently, the advancement of highly sensitive potential-controlled friction systems with superior potential response characteristics remains a top priority for future investigations.

Author Contributions: Writing—original draft preparation, S.L.; funding acquisition, S.L.; writing—review and editing, S.L., C.L., J.Z., X.Q. and Y.T.; formatting, review and re-editing, W.H., J.L., D.X., G.Q. and P.B.; review and supervision, Y.M. All authors have read and agreed to the published version of the manuscript.

Funding: This work was supported by the National Nature Science Foundation of China (no. 52275172) and Fundamental Research Funds for the Central Universities (no. FRF-TP-20-051A1).

Conflicts of Interest: The authors declare no conflict of interest.

References

- Luo, J.; Liu, M.; Ma, L. Origin of friction and the new frictionless technology—Superlubricity: Advancements and future outlook. *Nano Energy* **2021**, *86*, 106092. [CrossRef]
- Wen, S.; Huang, P. *Principles of Tribology*; John Wiley & Sons: Hoboken, NJ, USA, 2011.
- Persson, B.N.J.; Sivebaek, I.M.; Samoilov, V.N.; Zhao, K.; Volokitin, A.I.; Zhang, Z. On the origin of Amonton's friction law. *J. Phys. Condens. Matter* **2008**, *20*, 395006. [CrossRef]
- Ge, X.; Li, J.; Luo, J. Macroscale superlubricity achieved with various liquid molecules: A review. *Front. Mech. Eng.* **2019**, *5*, 2. [CrossRef]
- Wei, Y.; Li, S.; Huang, H.; Ding, C.; Wang, X. Experimental investigation on synergetic effects of micro grooves and WSe₂ in sliding contact. *Lubricants* **2022**, *10*, 208. [CrossRef]
- Rahman, M.H.; Warneke, H.; Webbert, H.; Rodriguez, J.; Austin, E.; Tokunaga, K.; Rajak, D.K.; Menezes, P.L. Water-based lubricants: Development, properties, and performances. *Lubricants* **2021**, *9*, 73. [CrossRef]
- Marian, M.; Tremmel, S. Current trends and applications of machine learning in tribology—a review. *Lubricants* **2021**, *9*, 86. [CrossRef]
- Vazirisereshk, M.R.; Martini, A.; Strubbe, D.A.; Baykara, M.Z. Solid lubrication with MoS₂: A review. *Lubricants* **2019**, *7*, 57. [CrossRef]
- Krim, J. Controlling friction with external electric or magnetic fields: 25 examples. *Front. Mech. Eng.* **2019**, *5*, 22. [CrossRef]
- Bhel, H.P. Tribology in electrical environments. *Lubr. Sci.* **2001**, *13*, 359–369. [CrossRef]
- Yang, X.; Meng, Y.; Tian, Y. Potential-controlled boundary lubrication of stainless steels in non-aqueous sodium dodecyl sulfate solutions. *Tribol. Lett.* **2014**, *53*, 17–26. [CrossRef]
- He, S.; Meng, Y.; Tian, Y. Correlation between adsorption/desorption of surfactant and change in friction of stainless steel in aqueous solutions under different electrode potentials. *Tribol. Lett.* **2011**, *41*, 485–494. [CrossRef]
- Li, R.; Zhang, X.R.; Zeng, C.; Yang, P.A.; Shou, M.J.; Zhu, D.; Lee, C.H. Magneto-controlled friction behaviors of magnetorheological elastomers with cosine-shaped surface structure. *Tribol. Int.* **2023**, *186*, 108658. [CrossRef]
- Kumar, S.; Sehgal, R.; Wani, M.F.; Sharma, M.D.; Ziyamukhamedova, U.; Dar, T.A. Next-generation ecofriendly mr fluid: Hybrid GO/ Fe₂O₃ encapsulated carbonyl iron microparticles with improved magnetorheological, tribological, and corrosion resistance properties. *Carbon* **2023**, *214*, 118331. [CrossRef]
- Ahamed, R.; Choi, S.B.; Ferdous, M.M. A state of art on magneto-rheological materials and their potential applications. *J. Intell. Mater. Syst. Struct.* **2018**, *29*, 2051–2095. [CrossRef]
- Babuska, T.F.; Pitenis, A.A.; Jones, M.R.; Nation, B.L.; Sawyer, W.G.; Argibay, N. Temperature-dependent friction and wear behavior of PTFE and MoS₂. *Tribol. Lett.* **2016**, *63*, 15. [CrossRef]
- Wu, Y.; Cai, M.; Pei, X.; Liang, Y.; Zhou, F. Switching friction with thermal-responsive gels. *Macromol. Rapid. Commun.* **2013**, *34*, 1785–1790. [CrossRef] [PubMed]
- Wu, Y.; Pei, X.; Wang, X.; Liang, Y.; Liu, W.; Zhou, F. Biomimicking lubrication superior to fish skin using responsive hydrogels. *NPG Asia Mater.* **2014**, *6*, e136. [CrossRef]
- De Wijn, A.S.; Fasolino, A.; Filippov, A.E.; Urbakh, M. Nanoscopic friction under electrochemical control. *Phys. Rev. Lett.* **2014**, *112*, 055502. [CrossRef]
- Sweeney, J.; Hausen, F.; Hayes, R.; Webber, G.B.; Endres, F.; Rutland, M.W.; Bennowitz, R.; Atkin, R. Control of nanoscale friction on gold in an ionic liquid by a potential-dependent ionic lubricant layer. *Phys. Rev. Lett.* **2012**, *109*, 155502. [CrossRef]
- Zhang, Y.B. Boundary lubrication—An important lubrication in the following time. *J. Mol. Liq.* **2006**, *128*, 56–59. [CrossRef]
- Stephan, S.; Schmitt, S.; Hasse, H.; Urbassek, H.M. Molecular dynamics simulation of the stribeck curve: Boundary lubrication, mixed lubrication, and hydrodynamic lubrication on the atomistic level. *Friction* **2023**, *11*, 2342–2366. [CrossRef]

23. Szeri, A.Z. *Fluid Film Lubrication: Theory and Design*; Cambridge University Press: Cambridge, UK, 1998.
24. Wong, P.L.; Bullough, W.A.; Feng, C.; Lingard, S. Tribological performance of a magneto-rheological suspension. *Wear* **2001**, *247*, 33–40. [[CrossRef](#)]
25. Feng, Y.P.; Su, J.S.; Cheng, H.B. Non-newtonian hydrodynamic modeling of electrorheological finishing feature based on wheel-like finishing tool. *J. Intell. Mater. Syst. Struct.* **2017**, *28*, 1407–1414. [[CrossRef](#)]
26. Melrose, J.R.; Itoh, S.; Ball, R.C. Simulations of electrorheological fluids with hydrodynamic lubrication. *Int. J. Mod. Phys. B* **1996**, *10*, 3211–3217. [[CrossRef](#)]
27. Kim, P.; Lee, J.I.; Seok, J. Analysis of a viscoplastic flow with field-dependent yield stress and wall slip boundary conditions for a magnetorheological (MR) fluid. *J. Non-Newton. Fluid Mech.* **2014**, *204*, 72–86. [[CrossRef](#)]
28. Wang, Y.S.; Wang, Q.J.; Lin, C.; Shi, F.H. Development of a set of stribeck curves for conformal contacts of rough surfaces. *Tribol. Trans.* **2006**, *49*, 526–535. [[CrossRef](#)]
29. Bowden, F.P.; Young, L. Influence of interfacial potential on friction and surface damage. *Res. J. Sci. Appl.* **1950**, *3*, 235–237.
30. Drummond, C. Electric-field-induced friction reduction and control. *Phys. Rev. Lett.* **2012**, *109*, 154302. [[CrossRef](#)]
31. Liu, C.; Li, X.; Li, X.; Li, W.; Tian, Y.; Meng, Y. On-line feedback control of sliding friction of metals lubricated by adsorbed boundary SDS films. *Lubricants* **2022**, *10*, 148. [[CrossRef](#)]
32. Tivony, R.; Zhang, Y.; Klein, J. Modulating interfacial energy dissipation via potential-controlled ion trapping. *J. Phys. Chem. C* **2021**, *125*, 3616–3622. [[CrossRef](#)]
33. Li, S.; Bai, P.; Li, Y.; Pesika, N.S.; Meng, Y.; Ma, L.; Tian, Y. Quantification/mechanism of interfacial interaction modulated by electric potential in aqueous salt solution. *Friction* **2021**, *9*, 513–523. [[CrossRef](#)]
34. Li, S.; Bai, P.; Li, Y.; Chen, C.; Meng, Y.; Tian, Y. Electric potential-controlled interfacial interaction between gold and hydrophilic/hydrophobic surfaces in aqueous solutions. *J. Phys. Chem. C* **2018**, *122*, 22549–22555. [[CrossRef](#)]
35. Cao, H.; Meng, Y. Electrochemical effect on boundary lubrication of zddp additive blended in propylene carbonate / diethyl succinate. *Tribol. Int.* **2018**, *126*, 229–239. [[CrossRef](#)]
36. Zhu, Y.Y.; Kelsall, G.H.; Spikes, H.A. The influence of electrochemical potentials on the friction and wear of iron and iron-oxides in aqueous systems. *Tribol. Trans.* **1994**, *37*, 811–819. [[CrossRef](#)]
37. Xie, G.; Guo, D.; Luo, J. Lubrication under charged conditions. *Tribol. Int.* **2015**, *84*, 22–35. [[CrossRef](#)]
38. Spikes, H.A. Triboelectrochemistry: Influence of applied electrical potentials on friction and wear of lubricated contacts. *Tribol. Lett.* **2020**, *68*, 90. [[CrossRef](#)]
39. Seed, C.M.; Acharya, B.; Krim, J. Qcm study of tribotronic control in ionic liquids and nanoparticle suspensions. *Tribol. Lett.* **2021**, *69*. [[CrossRef](#)]
40. Tysoe, W.T.; Spencer, N.D. Rapid testing of tribotronic materials. *Tribol. Lubr. Technol.* **2021**, *77*, 76–77.
41. Zhang, J.; Meng, Y.; Yu, X. Control of friction distribution on stainless steel surface in sodium dodecyl sulfate aqueous solution by bipolar electrochemistry. *Tribol. Lett.* **2015**, *59*, 43. [[CrossRef](#)]
42. Liu, C.; Fang, J.; Wen, X.; Tian, Y.; Meng, Y. Active control of boundary lubrication of ceramic tribo-pairs in sodium dodecyl sulfate aqueous solutions. *Tribol. Lett.* **2021**, *69*, 144. [[CrossRef](#)]
43. Zhu, Y.; Ogano, S.; Kelsall, G.; Spikes, H.A. The study of lubricant additive reactions using non-aqueous electrochemistry. *Tribol. Trans.* **2000**, *43*, 175–186. [[CrossRef](#)]
44. Xiaoyin, X. *Application of Electrochemical Techniques to Tribology*; Imperial College London (University of London): London, UK, 2004.
45. Edison, O. Improvement in Telegraph Apparatus. U.S. Patent 158,787, 9 January 1875.
46. American, N.J.S. The electromotograph. *A New Discov. Telegr.* **1874**, *31*, 145.
47. Pearson, B.R.; Brook, P.A.; Waterhouse, R.B. Influence of electrochemical potential on the wear of metals, particularly nickel. *Tribol. Int.* **1988**, *21*, 191–197. [[CrossRef](#)]
48. Kautek, W.; Dieluweit, S.; Sahre, M. Combined scanning force microscopy and electrochemical quartz microbalance in-situ investigation of specific adsorption and phase change processes at the silver/halogenide interface. *J. Phys. Chem. B* **1997**, *101*, 2709–2715. [[CrossRef](#)]
49. Labuda, A.; Hausen, F.; Gosvami, N.N.; Grütter, P.H.; Lennox, R.B.; Bennewitz, R. Switching atomic friction by electrochemical oxidation. *Langmuir* **2011**, *27*, 2561–2566. [[CrossRef](#)] [[PubMed](#)]
50. Liu, C.X.; Tian, Y.; Meng, Y.G. A chemical potential equation for modeling triboelectrochemical reactions on solid-liquid interfaces. *Front. Chem.* **2021**, *9*, 650880. [[CrossRef](#)] [[PubMed](#)]
51. Brandon, N.P.; Bonanos, N.; Fogarty, P.O.; Mahmood, M.N.; Moore, A.J.; Wood, R.J.K. Influence of potential on the friction and wear of mild-steel in a model aqueous lubricant. *J. Appl. Electrochem.* **1993**, *23*, 456–462. [[CrossRef](#)]
52. Ismail, M.N.F.; Harvey, T.J.; Wharton, J.A.; Wood, R.J.K.; Humphreys, A. Surface potential effects on friction and abrasion of sliding contacts lubricated by aqueous solutions. *Wear* **2009**, *267*, 1978–1986. [[CrossRef](#)]
53. Su, Y.Y. Electrochemical study of the interaction between fatty acid and oxidized copper. *Tribol. Int.* **1997**, *30*, 423–428. [[CrossRef](#)]
54. Su, Y.Y. Enhanced boundary lubrication by potential control during copper wire drawing. *Wear* **1997**, *210*, 165–170. [[CrossRef](#)]
55. Yang, X.; Meng, Y.; Tian, Y. Effect of imidazolium ionic liquid additives on lubrication performance of propylene carbonate under different electrical potentials. *Tribol. Lett.* **2014**, *56*, 161–169. [[CrossRef](#)]

56. Gosvami, N.N.; Bares, J.A.; Mangolini, F.; Konicek, A.R.; Yablon, D.G.; Carpick, R.W. Mechanisms of antiwear tribofilm growth revealed in situ by single-asperity sliding contacts. *Science* **2015**, *348*, 102–106. [[CrossRef](#)] [[PubMed](#)]
57. Liu, C.; Li, W.; Ouyang, C.; Tian, Y.; Meng, Y. Voltage-assisted tribofilm formation of sulfur- and phosphorus-free organic molybdenum additive on bearing steel surfaces in industrial base oils. *Tribol. Lett.* **2022**, *70*, 19. [[CrossRef](#)]
58. Liu, C.; Meng, Y.; Tian, Y. Potential-controlled boundary lubrication using mos2 additives in diethyl succinate. *Tribol. Lett.* **2020**, *68*, 72. [[CrossRef](#)]
59. Willermet, P.A.; Dailey, D.P.; Carter, R.O.; Schmitz, P.J.; Zhu, W. Mechanism of formation of antiwear films from zinc dialkyldithiophosphates. *Tribol. Int.* **1995**, *28*, 177–187. [[CrossRef](#)]
60. Xu, X.; Spikes, H. Study of zinc dialkyldithiophosphate in di-ethylhexyl sebacate using electrochemical techniques. *Tribol. Lett.* **2007**, *25*, 141–148. [[CrossRef](#)]
61. Wang, S.S.; Maheswari, S.P.; Tung, S.C. The nature of electrochemical reactions between several zinc organodithiophosphate antiwear additives and cast iron surfaces. *Tribol. Trans.* **1989**, *32*, 91–99. [[CrossRef](#)]
62. Tung, S.C.; Wang, S.S. In-situ electro-charging for friction reduction and wear resistant film formation. *Tribol. Trans.* **1991**, *34*, 479–488. [[CrossRef](#)]
63. Wang, S.S.; Tung, S.C. A reaction mechanism for producing low-friction iron phosphate coatings. *Tribol. Trans.* **1991**, *34*, 45–50. [[CrossRef](#)]
64. Xu, X.; Brandon, N.; Spikes, H. Study of zinc dialkyldithiophosphate using electrochemical techniques. In *Tribology Series*; Dowson, D., Priest, M., Dalmaz, G., Lubrecht, A.A., Eds.; Elsevier: Amsterdam, The Netherlands, 2002; pp. 175–181.
65. Klein, J. Hydration lubrication. *Friction* **2013**, *1*, 1–23. [[CrossRef](#)]
66. He, S.; Meng, Y.; Tian, Y. Effects of the concentration of sodium lauryl sulfate solution and NaCl additive on the potential-controlled friction. In *Advanced Tribology*; Luo, J., Meng, Y., Shao, T., Zhao, Q., Eds.; Springer: Berlin/Heidelberg, Germany, 2010; pp. 408–412.
67. Brandon, N.P.; Bonanos, N.; Fogarty, P.O.; Mahmood, M.N. The effect of interfacial potential on friction in a model aqueous lubricant. *J. Electrochem. Soc.* **1992**, *139*, 3489–3492. [[CrossRef](#)]
68. He, S.; Meng, Y.; Tian, Y.; Zuo, Y. Response characteristics of the potential-controlled friction of ZrO₂/stainless steel tribopairs in sodium dodecyl sulfate aqueous solutions. *Tribol. Lett.* **2010**, *38*, 169–178. [[CrossRef](#)]
69. Zhang, J.; Meng, Y.; Tian, Y.; Zhang, X. Effect of concentration and addition of ions on the adsorption of sodium dodecyl sulfate on stainless steel surface in aqueous solutions. *Colloids Surf. A* **2015**, *484*, 408–415. [[CrossRef](#)]
70. Gao, T.; Li, J.; Wang, W.; Luo, J. Extremely low friction on gold surface with surfactant molecules induced by surface potential. *Friction* **2022**, *11*, 513–523. [[CrossRef](#)]
71. Jacob, N. *Israelachvili. Intermolecular and Surface Forces*, 3rd ed.; Academic Press: Burlington, MA, USA, 2011; pp. 59–65.
72. Han, T.; Zhang, S.; Zhang, C. Unlocking the secrets behind liquid superlubricity: A state-of-the-art review on phenomena and mechanisms. *Friction* **2022**, *10*, 1137–1165. [[CrossRef](#)]
73. Han, T.; Zhao, M.; Sun, C.; Zhao, R.; Xu, W.; Zhang, S.; Zhang, C. Macroscale superlubricity of hydrated anions in the boundary lubrication regime. *ACS Appl. Mater. Interfaces* **2023**, *15*, 42094–42103. [[CrossRef](#)] [[PubMed](#)]
74. Han, T.Y.; Cao, W.; Xu, Z.; Adibnia, V.; Olgiati, M.; Valtiner, M.; Ma, L.; Zhang, C.; Ma, M.; Luo, J.; et al. Hydration layer structure modulates superlubrication by trivalent La³⁺ electrolytes. *Sci. Adv.* **2023**, *9*, eadf3902. [[CrossRef](#)] [[PubMed](#)]
75. Gao, T.; Li, J.; Yi, S.; Luo, J. Potential-dependent friction on a graphitic surface in ionic solution. *J. Phys. Chem. C* **2020**, *124*, 23745–23751. [[CrossRef](#)]
76. Noguchi, H.; Okada, T.; Uosaki, K. Sfg study on potential-dependent structure of water at pt electrode/electrolyte solution interface. *Electrochim. Acta* **2008**, *53*, 6841–6844. [[CrossRef](#)]
77. Velasco-Velez, J.J.; Wu, C.H.; Pascal, T.A.; Wan, L.W.F.; Guo, J.H.; Prendergast, D.; Salmeron, M. The structure of interfacial water on gold electrodes studied by x-ray absorption spectroscopy. *Science* **2014**, *346*, 831–834. [[CrossRef](#)]
78. Guriyanova, S.; Mairanovsky, V.G.; Bonaccorso, E. Superviscosity and electroviscous effects at an electrode/aqueous electrolyte interface: An atomic force microscope study. *J. Colloid. Interface Sci.* **2011**, *360*, 800–804. [[CrossRef](#)] [[PubMed](#)]
79. Plausinaitis, D.; Pulmanas, A.; Kubilius, V.; Raudonis, R.; Daujotis, V. Properties of an interfacial solution layer at gold electrode surface in perchlorate and chloride solutions: Piezoelectric resonator and drag force study. *Electrochim. Acta* **2014**, *121*, 278–284. [[CrossRef](#)]
80. Pashazanusi, L.; Oguntoye, M.; Oak, S.; Albert, J.N.L.; Pratt, L.R.; Pesika, N.S. Anomalous potential-dependent friction on Au(111) measured by afm. *Langmuir* **2018**, *34*, 801–806. [[CrossRef](#)] [[PubMed](#)]
81. Pashazanusi, L.; Kristiansen, K.; Li, S.; Tian, Y.; Pesika, N.S. Role of interfacial water and applied potential on friction at Au(111) surfaces. *Front. Mech. Eng.* **2019**, *5*, 39. [[CrossRef](#)]
82. Li, S.; Li, Y.; Bai, P.; Meng, Y.; Tian, Y. Potential-dependent interfacial frictional behavior between charged microspheres and gold in aqueous solutions. *J. Phys. Chem. C* **2022**, *126*, 4555–4562. [[CrossRef](#)]
83. Liu, Y.; Li, J.; Chen, X.; Luo, J. Fluorinated graphene: A promising macroscale solid lubricant under various environments. *ACS Appl. Mater. Interfaces* **2019**, *11*, 40470–40480. [[CrossRef](#)] [[PubMed](#)]
84. Liu, C.; Friedman, O.; Li, Y.; Li, S.; Tian, Y.; Golan, Y.; Meng, Y. Electric response of cus nanoparticle lubricant additives: The effect of crystalline and amorphous octadecylamine surfactant capping layers. *Langmuir* **2019**, *35*, 15825–15833. [[CrossRef](#)] [[PubMed](#)]

85. Mou, Z.; Peng, J.; Yan, R.; Yang, Q.; Zhao, B.; Xiao, D. Electrical stimulation enables dynamic regulation of the tribological behaviors of polyelectrolyte-modified carbon dots. *Carbon* **2023**, *203*, 11–20. [[CrossRef](#)]
86. Guo, Y.; Zhang, L.; Zhang, G.; Wang, D.; Wang, T.; Wang, Q. High lubricity and electrical responsiveness of solvent-free ionic SiO_2 nanofluids. *J. Mater. Chem. A* **2018**, *6*, 2817–2827. [[CrossRef](#)]
87. Seed, C.M.; Acharya, B.; Nunn, N.; Smirnov, A.I.; Krim, J. Tribotronic and electrochemical properties of platinum–nanofluid interfaces formed by aqueous suspensions of 5 and 40 nm TiO_2 nanoparticles. *J. Chem. Phys.* **2023**, *159*, 114705. [[CrossRef](#)]
88. Seed, C.M.; Acharya, B.; Perelygin, V.; Smirnov, A.I.; Krim, J. Tribotronic control and cyclic voltammetry of platinum interfaces with metal oxide nanofluids. *Appl. Surf. Sci.* **2021**, *566*, 150675. [[CrossRef](#)]
89. Hayes, R.; Warr, G.G.; Atkin, R. Structure and nanostructure in ionic liquids. *Chem. Rev.* **2015**, *115*, 6357–6426. [[CrossRef](#)] [[PubMed](#)]
90. Dong, K.; Liu, X.; Dong, H.; Zhang, X.; Zhang, S. Multiscale studies on ionic liquids. *Chem. Rev.* **2017**, *117*, 6636–6695. [[CrossRef](#)] [[PubMed](#)]
91. Rakov, D.A.; Chen, F.F.; Ferdousi, S.A.; Li, H.; Pathirana, T.; Simonov, A.N.; Howlett, P.C.; Atkin, R.; Forsyth, M. Engineering high-energy-density sodium battery anodes for improved cycling with superconcentrated ionic-liquid electrolytes. *Nat. Mater.* **2020**, *19*, 1096–1101. [[CrossRef](#)] [[PubMed](#)]
92. Forsyth, M.; Porcarelli, L.; Wang, X.; Goujon, N.; Mecerreyes, D. Innovative electrolytes based on ionic liquids and polymers for next-generation solid-state batteries. *Acc. Chem. Res.* **2019**, *52*, 686–694. [[CrossRef](#)] [[PubMed](#)]
93. Lhermerout, R.; Diederichs, C.; Perkin, S. Are ionic liquids good boundary lubricants? A molecular perspective. *Lubricants* **2018**, *6*, 9. [[CrossRef](#)]
94. Di Lecce, S.; Kornyshev, A.A.; Urbakh, M.; Bresme, F. Electrotunable lubrication with ionic liquids: The effects of cation chain length and substrate polarity. *ACS Appl. Mater. Interfaces* **2020**, *12*, 4105–4113. [[CrossRef](#)]
95. Perkin, S.; Albrecht, T.; Klein, J. Layering and shear properties of an ionic liquid, 1-ethyl-3-methylimidazolium ethylsulfate, confined to nano-films between mica surfaces. *Phys. Chem. Chem. Phys.* **2010**, *12*, 1243–1247. [[CrossRef](#)]
96. Li, H.; Wood, R.J.; Rutland, M.W.; Atkin, R. An ionic liquid lubricant enables superlubricity to be “switched on” in situ using an electrical potential. *Chem. Commun.* **2014**, *50*, 4368. [[CrossRef](#)]
97. Li, H.; Rutland, M.W.; Watanabe, M.; Atkin, R. Boundary layer friction of solvate ionic liquids as a function of potential. *Faraday Discuss* **2017**, *199*, 311–322. [[CrossRef](#)]
98. Kong, L.L.; Huang, W.; Wang, X.L. Ionic liquid lubrication at electrified interfaces. *J. Phys. D Appl. Phys.* **2016**, *49*. [[CrossRef](#)]
99. Cooper, P.K.; Li, H.; Rutland, M.W.; Webber, G.B.; Atkin, R. Tribotronic control of friction in oil-based lubricants with ionic liquid additives. *Phys. Chem. Chem. Phys.* **2016**, *18*, 23657–23662. [[CrossRef](#)]
100. Pilkington, G.A.; Oleshkevych, A.; Pedraz, P.; Watanabe, S.; Radiom, M.; Reddy, A.B.; Vorobiev, A.; Glavatskin, S.; Rutland, M. Electroresponsive structuring and friction of a non-halogenated ionic liquid in a polar solvent: Effect of concentration. *Phys. Chem. Chem. Phys.* **2020**, *22*, 19162–19171. [[CrossRef](#)]
101. Gatti, F.; Amann, T.; Kailer, A.; Baltes, N.; Ruhe, J.; Gumbsch, P. Towards programmable friction: Control of lubrication with ionic liquid mixtures by automated electrical regulation. *Sci. Rep.* **2020**, *10*, 17634. [[CrossRef](#)] [[PubMed](#)]
102. Antognozzi, M.; Humphris, A.D.L.; Miles, M.J. Observation of molecular layering in a confined water film and study of the layers viscoelastic properties. *Appl. Phys. Lett.* **2001**, *78*, 300–302. [[CrossRef](#)]
103. Gao, Y.; Xue, B.; Ma, L.; Luo, J. Effect of liquid crystal molecular orientation controlled by an electric field on friction. *Tribol. Int.* **2017**, *115*, 477–482. [[CrossRef](#)]
104. Amann, T.; Kailer, A. Relationship between ultralow friction of mesogenic-like fluids and their lateral chain length. *Tribol. Lett.* **2011**, *41*, 121–129. [[CrossRef](#)]
105. Amann, T.; Dold, C.; Kailer, A. Rheological characterization of ionic liquids and ionic liquid crystals with promising tribological performance. *Soft Matter* **2012**, *8*, 9840–9846. [[CrossRef](#)]
106. Olivero, D.; Evangelista, L.R.; Barbero, G. External electric-field effect on nematic anchoring energy. *Phys. Rev. E* **2002**, *65*, 031721. [[CrossRef](#)]
107. Nastishin, Y.A.; Polak, R.D.; Shiyanovskii, S.V.; Bodnar, V.H.; Lavrentovich, O.D. Nematic polar anchoring strength measured by electric field techniques. *J. Appl. Phys.* **1999**, *86*, 4199–4213. [[CrossRef](#)]
108. Mori, S.; Iwata, H. Relationship between tribological performance of liquid crystals and their molecular structure. *Tribol. Int.* **1996**, *29*, 35–39. [[CrossRef](#)]
109. Kimura, Y.; Nakano, K.; Kato, T.; Morishita, S. Control of friction coefficient by applying electric fields across liquid crystal boundary films. *Wear* **1994**, *175*, 143–149. [[CrossRef](#)]
110. Morishita, S.; Nakano, K.; Kimura, Y. Electroviscous effect of nematic liquid crystals. *Tribol. Int.* **1993**, *26*, 399–403. [[CrossRef](#)]
111. Manzato, C.; Foster, A.S.; Alava, M.J.; Laurson, L. Friction control with nematic lubricants via external fields. *Phys. Rev. E* **2015**, *91*, 012504. [[CrossRef](#)] [[PubMed](#)]
112. Klein, J. Shear, friction, and lubrication forces between polymer-bearing surfaces. *Annu. Rev. Mater. Sci.* **1996**, *26*, 581–612. [[CrossRef](#)]
113. Zeng, H.; Zhang, Y.; Mao, S.; Nakajima, H.; Uchiyama, K. A reversibly electro-controllable polymer brush for electro-switchable friction. *J. Mater. Chem. C* **2017**, *5*, 5877–5881. [[CrossRef](#)]

114. Li, H.; Zhang, Y.; Jones, S.; Segalman, R.; Warr, G.G.; Atkin, R. Interfacial nanostructure and friction of a polymeric ionic liquid-ionic liquid mixture as a function of potential at Au(1 1 1) electrode interface. *J. Colloid. Interface Sci.* **2022**, *606*, 1170–1178. [[CrossRef](#)]
115. Gatti, F.J.; Cai, W.H.; Herzog, R.; Gharavian, A.; Kailer, A.; Baltés, N.; Rabenecker, P.; Mörchel, P.; Balzer, B.N.; Amann, T.; et al. Investigation of programmable friction with ionic liquid mixtures at the nano- and macroscales. *Lubricants* **2023**, *11*, 376. [[CrossRef](#)]
116. Gatti, F.; Amann, T.; Kailer, A.; Abicht, J.; Rabenecker, P.; Baltés, N.; Rühle, J. Makroskopische reibwertsteuerung durch elektrochemische potenziale mit ionischen flüssigkeiten: Makroskopische reibwertsteuerung durch elektrochemische potenziale mit ionischen flüssigkeiten. *Tribol. Und Schmier.* **2019**, *66*, 51–57.
117. Kawada, S.; Ogawa, S.; Sasaki, S.; Miyatake, M. Friction control by applying electric potential under lubrication with ionic liquids. *Tribol. Online* **2019**, *14*, 71–77. [[CrossRef](#)]
118. Guo, Y.; Liu, G.; Li, G.; Zhao, F.; Zhang, L.; Guo, F.; Zhang, G. Solvent-free ionic silica nanofluids: Smart lubrication materials exhibiting remarkable responsiveness to weak electrical stimuli. *Chem. Eng. J.* **2020**, *383*, 123202. [[CrossRef](#)]
119. Michalec, M.; Svoboda, P.; Krupka, I.; Hartl, M.; Vencl, A. Investigation of the tribological performance of ionic liquids in non-conformal ehl contacts under electric field activation. *Friction* **2020**, *8*, 982–994. [[CrossRef](#)]
120. Zhang, C.; Chen, J.; Liu, M.; Wang, F.; Zheng, Y.; Cheng, Y.; Liu, Z. Relationship between viscosity and resistance of oil film: A new way to investigate the controllable friction between charged interfaces lubricated by ionic lubricating oil. *Adv. Mater. Interfaces* **2022**, *9*, 2200229. [[CrossRef](#)]
121. Ulrich, C.; Andersson, O.; Nyholm, L.; Björefors, F. Formation of molecular gradients on bipolar electrodes. *Angew. Chem. Int. Ed.* **2008**, *47*, 3034–3036. [[CrossRef](#)] [[PubMed](#)]
122. Ulrich, C.; Andersson, O.; Nyholm, L.; Björefors, F. Potential and current density distributions at electrodes intended for bipolar patterning. *Anal. Chem.* **2009**, *81*, 453–459. [[CrossRef](#)] [[PubMed](#)]
123. Hsu, S.; Ying, C.; Zhao, F. The nature of friction: A critical assessment. *Friction* **2014**, *2*, 1–26. [[CrossRef](#)]
124. Kelsall, G.H.; Zhu, Y.; Spikes, H.A. Electrochemical effects on friction between metal oxide surfaces in aqueous solutions. *J. Chem. Soc. Faraday Trans.* **1993**, *89*, 267–272. [[CrossRef](#)]
125. Alkan, S.; Gök, M.S. Effect of sliding wear and electrochemical potential on tribocorrosion behaviour of AISI 316 stainless steel in seawater. *Eng. Sci. Technol.* **2021**, *24*, 524–532. [[CrossRef](#)]
126. Bonanos, N.; Brandon, N.P.; Mahmood, M.N.; Brown, D. The effect of imposed electrical current on torque release at the metal-mudcake interface. *J. Appl. Electrochem.* **1996**, *26*, 977–980. [[CrossRef](#)]
127. Brandon, N.P.; Wood, R.J.K. The influence of interfacial potential on friction and wear in an aqueous drilling mud. *Wear* **1993**, *170*, 33–38. [[CrossRef](#)]
128. Sun, Y.; Song, C.; Liu, Z.; Li, J.; Wang, L.; Sun, C.; Zhang, Y. Tribological and conductive behavior of Cu/Cu rolling current-carrying pairs in a water environment. *Tribol. Int.* **2020**, *143*, 106055. [[CrossRef](#)]
129. Sun, Y.; Song, C.; Liu, Z.; Li, J.; Sun, Y.; Shangguan, B.; Zhang, Y. Effect of relative humidity on the tribological/conductive properties of cu/cu rolling contact pairs. *Wear* **2019**, *436–437*, 203023. [[CrossRef](#)]
130. Hu, B.; Meng, Y.; Wen, S. A preliminary experimental study on voltage-controlled friction clutch. *Tribology* **2004**, *24*, 46–50.
131. Wenjie, Z. Research progress in tribo-electrochemistry and tribo-electrochemical polishing. *Tribology* **2006**, *26*, 92–96.
132. Li, C.H.; Wang, R.J.; Seiler, J.; Bhat, I. Electro-chemical mechanical polishing of silicon carbide. *Mater. Sci. Forum.* **2004**, *33*, 481–486.
133. Zhai, W.; Wang, C. Study on characteristics and mechanism of silicon nitride in electrochemical grinding. *Tribology* **2004**, *24*, 360–363.
134. He, Y.; She, D.; Liu, Z.; Wang, X.; Zhong, L.; Wang, C.; Wang, G.; Mao, S.X. Atomistic observation on diffusion-mediated friction between single-asperity contacts. *Nat. Mater.* **2022**, *21*, 173–180. [[CrossRef](#)]

Disclaimer/Publisher’s Note: The statements, opinions and data contained in all publications are solely those of the individual author(s) and contributor(s) and not of MDPI and/or the editor(s). MDPI and/or the editor(s) disclaim responsibility for any injury to people or property resulting from any ideas, methods, instructions or products referred to in the content.